คุณลักษณะของตัวเร่งปฏิกิริยา W/ZrO_2 ที่เซอร์โคเนียถูกปรับปรุงด้วยแกลเลียมและโบรอน สำหรับเอสเทอริฟิเคชัน

นางสาวชนิดาภา ผดุงพิทักษ์ชน

วิทยานิพนธ์นี้เป็นส่วนหนึ่งของการศึกษาตามหลักสูตรปริญญาวิศวกรรมศาสตร์มหาบัณฑิต
สาขาวิชาวิศวกรรมเคมี ภาควิชาวิศวกรรมเคมี
คณะวิศวกรรมศาสตร์ จุฬาลงกรณ์มหาวิทยาลัย
ปีการศึกษา 2556

CHARACTERISTIC OF GALLIUM AND BORON MODIFIED ZrO_2 ON W/ZrO_2 CATALYST FOR ESTRIFICATION

Miss Chanidapa Padoongpitukchon

A Thesis Submitted in Partial Fulfillment of the Requirements
for the Degree of Master of Engineering Program in Chemical Engineering
Department of Chemical Engineering
Faculty of Engineering
Chulalongkorn University
Academic Year 2013

Thesis Title	CHARACTERISTIC OF GALLIUM AND BORON MODIFIED ZrO_2 ON W/ZrO_2 CATALYST FOR ESTERIFICATION
By	Miss Chanidapa Padoongpitukchon
Field of Study	Chemical Engineering
Thesis Advisor	Associate Professor Bunjerd Jongsomjit, Ph.D.

Accepted by the Faculty of Engineering, Chulalongkorn University in Partial Fulfillment of the Requirements for the Master's Degree

.....Dean of the Faculty of Engineering
(Associate Professor Boonsom Lerdirungwong, Dr.Ing.)

THESIS COMMITTEE

.....Chairman
(Associate Professor Muenduen Phisalaphong, Ph.D.)

.....Thesis Advisor
(Associate Professor Bunjerd Jongsomjit, Ph.D.)

.....Examiner
(Chutimon Satirapipathkul, Ph.D.)

.....External Examiner
(Ekrachan Chaichana, D.Eng.)

ชนิดาภา ผดุงพิทักษ์ชน : คุณลักษณะของตัวเร่งปฏิกิริยา W/ZrO_2 ที่เซอร์โคเนียถูกปรับปรุงด้วยแกลเลียมและโบรอนสำหรับเอสเทอริฟิเคชัน.(CHARACTERISTIC OF GALLIUM AND BORON MODIFIED ZrO_2 ON W/ZrO_2 CATALYSTS FOR ESTERIFICATION) อ.ที่ปรึกษาวิทยานิพนธ์หลัก : รศ.ดร. บรรเจิด จงสมจิตร , 70 หน้า.

วิธีการโซลโวลเทอร์มอลและวิธีการตกตะกอนถูกนำมาใช้สำหรับการเตรียมตัวรองรับเซอร์โคเนีย หลังจากนั้นตัวรองรับเซอร์โคเนียจะถูกฝังเคลือบกับทังสเตนคลอไรด์เพื่อให้ได้ตัวเร่งปฏิกิริยา W/ZrO_2 โดยพบว่าวิธีการเตรียมแบบโซลโวลเทอร์มอลนั้นรูปร่างของเซอร์โคเนียที่ได้มีลักษณะเป็นทรงกลมและมีมวลหนาแน่น ส่วนวิธีการตกตะกอนนั้นพบว่าตัวอย่างที่ได้มีความขรุขระของอนุภาค ผล XRD ของตัวเร่งปฏิกิริยา W/ZrO_2 แสดงโมโนไคนิค, เตตระโกนอลของเซอร์โคเนียและผลึกทังสเตนออกไซด์ WO_3 บนทั้งสองวิธีการเตรียม โดยได้รับการยืนยันด้วยวิธีรามาน โดยตัวเร่งปฏิกิริยาแสดงการกระจายตัวที่ดีของ WO_x โดยแสดงผล polytungstate บนพื้นผิวของตัวเร่งปฏิกิริยาและยังมีการรวมตัวกันของ WO_3 ร่วมกับ polytungstate บนพื้นผิวอีกด้วย โดยพื้นผิวของวิธีการเตรียมด้วยวิธีการตกตะกอนนั้นให้พื้นที่ผิวที่มากที่สุดซึ่งส่งผลต่อความว่องไวของตัวเร่งปฏิกิริยาในปฏิกิริยาเอสเทอริฟิเคชันที่ดีที่สุดด้วย สำหรับการปรับปรุงแกลเลียมด้วยแกลเลียมไนเตรทที่ 0.5 และ 1 โดยน้ำหนักบนตัวรองรับเซอร์โคเนียนั้น รูปร่างของตัวรองรับไม่มีเปลี่ยนแปลงหลังจากที่ฝังเคลือบ โดยพื้นที่ผิวและความเป็นกรดของตัวปรับปรุงแกลเลียมสูงกว่าที่ไม่ปรับปรุง และตัวเร่งปฏิกิริยาที่มีปรับปรุงด้วยแกลเลียม 1 เปอร์เซ็นต์โดยน้ำหนักด้วยวิธีการตกตะกอน (W/ZrO2_1% Ga_pre) ให้ประสิทธิภาพการทำงานของตัวเร่งปฏิกิริยาสูงที่สุด สำหรับการปรับปรุงโบรอนด้วยกรดบอริกที่ 0.5 และ 1 โดยน้ำหนักบนตัวรองรับเซอร์โคเนียนั้นพบว่าพื้นที่ผิวและความเป็นกรดของตัวรองรับมีค่าสูงขึ้นหลังจากฝังเคลือบด้วยโบรอน อย่างไรก็ตามผลที่เกิดหลังจากเคลือบด้วยทังสเตนแสดงให้เห็นแนวโน้มตรงข้าม โดยที่การฝังเคลือบด้วยโบรอนนั้น ความว่องไวและความเป็นกรดลดลงมากกว่าตัวที่ไม่ได้ปรับปรุงซึ่งมีผลกระทบทั้งสองวิธีการเตรียม เหตุผลที่เป็นไปได้อาจจะเป็นเพราะขนาดอะตอมของโบรอนที่มีขนาดเล็กนั้นมีผลกระทบต่อทังสเตนแล้วส่งผลให้ความเป็นกรดลดลง

ภาควิชา วิศวกรรมเคมี ลายมือชื่อนิสิต .....

สาขาวิชา วิศวกรรมเคมี ลายมือชื่อ อ.ที่ปรึกษาวิทยานิพนธ์หลัก .....

ปีการศึกษา 2556 .....

5471019421 : MAJOR CHEMICAL ENGINEERING
KEYWORDS : TUNSTATED ZIRCONIA / ESTERIFICATION / SOLVOTHERMAL / PRECIPITATION / GALLIUIM / BORON / SOLID ACID CATALYST

CHANIDAPA PADOONGPITUKCHON : CHARACTERISTIC OF GALLIUM AND BORON MODIFIED ZrO_2 ON W/ZrO_2 CATALYST FOR ESTERIFICATION. ADVISOR : ASSOCIATE PROFESSOR BUNJERD JONGSOMJIT, Ph.D., 70 pp.

The solvothermal and precipitation methods were used for the preparation of zirconia (ZrO_2). Then, the ZrO_2 supports were impregnated with tungsten (VI) chloride to obtain W/ZrO_2 catalyst. It was found that the spherical shape and dense mass in solvolthermal sample and irregular roughness shape particle in precipitation method were obtained. The XRD results of W/ZrO_2 presented the monoclinic, tetragonal zirconia and WO_3 crystalline for both preparation methods, which can be confirmed with the raman spectroscopy. The resulting catalysts exhibited good dispersion of WOx species as surface polytungstates on these catalysts and also have agglomeration of WO_3 together with polytungstate. The BET surface area of precipitation method was the highest and affected on high catalytic performance on esterification. For the Ga modification from $GaNO_3$ with 0.5wt% and 1wt% on the zirconia support, the morphology was not changed after impregnation. The surface area and surface acidity of the Ga-modified zirconia support was higher than the unmodified one. The catalyst having 1 wt% of Ga with precipitation method (W/ZrO_2_1%Ga_pre) also gave high catalytic performance. For the B modification from HBO_3 with 0.5wt% and 1wt% on the zirconia support, the surface acidity and BET surface of the zirconia are higher after impregnation with boron. However, the results after impregnated with tungsten showed the opposite trend. With boron loading the activity and surface acidity decreased than the unmodified one, affecting by the two preparation methods. The possible reason may be the small atomic size of boron is able to interact with tungsten resulting in the decreased surface acidity.

Department : Chemical Engineering Student's Signature .....

Field of Study : Chemical Engineering Advisor's Signature .....

Academic Year : 2013

ACKNOWLEDGEMENTS

First of all, I would like appreciate my advisor, Assistance professor Bunjerd Jongsomjit, to get me on the path to this master degree. His encouragement and faith in me throughout have been extremely helpful. He was available for my questions and he was positive and gave generously of his time and vast knowledge. I am also grateful to thank Assistance Professor Dr. Muenduen Phisalaphong for chairman, Dr. Chutimon Satirapipathkul and Dr.Ekrachan Chaichana for kindly serving as my committee members including valuable suggestions and comment.

Many thanks for kind suggestions and useful help to Miss Sasiradee Jantasee, Miss Nuttakarn Jungjitamet and many friends in the Center of Excellence on Catalysis from Chulalongkorn University who always provided the co-operate along the thesis study.

I would like to express my deepest appreciation to Miss Punyawee Reaungart who to give me a chance to study in master degree of chemical engineering at Chulalongkorn University and give me a support during the course, including my colleagues (Advance Engineer team) who always gave me an encouragement.

Most of all, I would like to express my greatest gratitude to my parents and my family who always beside me all the times. Thank you for all suggestions, support and encouragement.

CONTENTS

LIST OF TABLES

LIST OF FIGURES

Page

Page

CHAPTER I

INTRODUCTION

Currently, there is a great interest in the biodiesel because of its many advantage and represents a promising renewable of energy source. Biodiesel can be chemically defined as a fuel composed of mono-alkyl esters of long chain fatty acids derived from renewable sources, such as vegetable oils and animal fats [1]. It is well known that the direct use of vegetable oils in internal combustion engine is problematic. These vegetable oils do not burn completely due to contain free fatty acids (FFA) at high level in oils. Free fatty acids have influence to undesirable saponification and leading to low product yields and complication in the subsequent separation steps [2]. An improvement on pre-treatment for disposal free fatty acids at an esterification step is required in which preliminary process of biodiesel production.

The homogeneous acid catalysts has been usually present excellent reaction yields such as H_2SO_4, HCL, HF, H_3PO_4 and etc but new problems arose, such as difficult separation from the reaction medium and serious environmental and corrosion-related problems [3]. It has including the cause of lead to serious contamination problem that make essential the implementation of product purification protocols. Then, the use of solid acid catalyst offer many advantages over exiting homogeneous catalyst used in biodiesel synthesis. There have been several reports on the generation of solid acid catalysts especially the catalyst which have zirconia supported.

In particular the most typical ones such as sulfated zirconia (SO_4/ZrO_2) and Tungstated zirconia (WO_3/ZrO_2) have been reported to have the potential for biodiesel synthesis as esterification and teanesterification. Sulfated zirconia is has been widely used for various reactions because super-acid catalyst [4]. Although sulphated zirconia has the highest acidity of solid super-acids but this catalyst has still limited such relative small surface [5], leaching and deactication [6]. Tungstated zirconia

(WO_3/ZrO_2) is a solid superacid same as sulfated zirconia. It has high catalytic activity in a proton transfer [7]. López *et al.,* [8] studied calcine temperature effect to S/Z, W/Z and Ti/Z. It revealed that SZ500 shows highest activity toward esterification than W/Z800 and TiZ500. In catalyst reusability, they suggest WZ are stable than SZ catalyst in long term due to the decrease in the reaction rate to sulfur leaching, poisoning.

Tungstated zirconia is structurally more stable than sulfated zirconia [9]. Thus, giving more steady performance in catalysis, it is also less active [10]. Moreover, improving the catalytic activity of tungstated zirconia catalyst is much attention because catalytic activity of tungstated zirconia can be improved by progressive acid modified, which results in the enhancement of surface area and surface acidity. It is well known that the esterification process is much required proton donated from acid. Then, The boron and gallium modified zirconium dioxides have interesting to modified on tungstated zirconia catalyst for improve catalytic activities. By, the boric acid and gallium are modified in several catalyst such as Ni-based catalyst for hydrogenation [11] hydrodesulfurization activity of $MoS_2/Al2O_3$ and Co–$MoS_2/Al2O_3$ catalysts [12], steam reforming over Ni/Ga/Mg/Zeolite Y catalysts [13], Ga-MCM-22 in isobuane production [14]

In present study, we investigated the catalytic performance for esterification of the promotion effect of impregnation of boron and gallium on ZrO_2. In addition to, the effect of preparation of zirconia samples by solvothermal and precipitation was determined. All the different treated zirconia samples were characterized by means of XRD, and Raman spectroscopy. The W/ZrO_2 and modified $W\text{-}ZrO_2$ catalysts were tested via esterification of acetic acid and methanol under the same reaction conditions.

The objectives of these research are following.

1. To investigate the effect of preparation method to synthesize ZrO_2 support.
2. To investigate the effect of content of boron and gallium added in ZrO_2 on the physicochemical properties of ZrO_2.
3. To investigate the characteristic and the catalytic properties of different W/ZrO_2 catalyst.
4. To investigate the characteristic and the catalytic properties of B and Ga modified zirconia supports.
5. To investigate the activity of catalysts via liquid phase esterification at atmospheric pressure.

By following the research objective, the scope of research as follows:

1. Preparation of ZrO_2 by precipitation method and solvolthermal method.
2. Preparation of acid increased on ZrO2 by impregnation with boron and Gallium.
3. Preparation of ZrO_2 supported W catalyst (15wt% of W) using the incipient wetness impregnation method.
4. Characterization of the catalyst sample using X-ray diffraction (XRD), BET surface area, Raman spectroscopy, acidity measurement, etc
5. Study of catalytic activity in liquid phase esterification at atmospheric pressure.

The benefits of these research are as follows.

1. Comparison catalysts of Ga and B-modified ZrO_2 on W/ZrO_2 catalysts for esterification.
2. To understand the effect of acid characteristic on boron and gallium for esterification.
3. To develop esterification by improve proper catalysts.

Chapter II

Literature review

2.1 Tungstated zirconia catalyst

Tungstated zirconia [WO_x/ZrO_2 (WZ)] catalysst have been extensicely studies in a past few years of their physical properties and their ability as catalyst for isomerization [15, 16], hydroisomerization, alkane conversion [17], especially tranesterification and esterification [18]. WO_x/ZrO_2 catalysts are advantage more than another modifier which was reported by López *et al.,* [8] al that WZ was found to be the suitable and active than TIZ and SZ for esterification. WZ can be easily regenerate than SZ .

Most of literature have attention to study the characteristics of [WO_x/ZrO_2 (WZ)] nanoparticle due to the influence to the activities came from surface densities of nanoparticle depending on the preparing method. It is well known calcination and tungsten loading preparation are the main preparation factor effect to surface densities.

López *et al.,* [18] studied the effect of calcaination temperature on esterification and tranesterification using zirconia. They studied the esterification of acetic (in both the gas and liquid phase) and the tranesterification of triaetin (a synthetic triglyceride in the liquid phase) with methanol by varying the calcination temperature at 400^oC-900^oC. It can be concluded that at moderate calcination temperature (500^oC – 800^oC) it contained primarily the tetragonal phase of zirconia (t-ZrO_2) when increased the calcination temperature it presented the monoclinic phase of zirconia and crystal WO_3. The increase in esterification and tranesterification catalyst activity coincide with the formation of polymeric tungsten species in the presence of the tetragonal phase of the ZrO_2 support. The activity drop at high WO_x surface densities is attributed to the loss of active sites. It result is consistent with the work of

Rabindran and co-worker [19] reported that percent_tetragonal phase decreases as the calcination temperature increases to 1073K and the ascribe to WO_3 crytallites increase with an increase in calcination temperature to1123K. Kaucký *et al*.,[20] conclude that beside the diffractions corresponding to tetragonal and monoclinic ZrO_2 phase have crystallites expected of low surface area.

There have been several studies on the role of tungstated loading, For instance, Parida *et al*., [21] studied the effect of W concentration and activation temperature of the catalyst with a series of WO_x/ZrO_2 samples that varying concentrations of W (10-25wt.%) prepared and activated at 650 and 750^oC. The XRD result at 15wt% showed the tetragonal phase of zirconia. However, above and less than 15wt.% shows peak corresponding to monoclinic WO_3 and monoclinic ZrO_2. Sakthivel *et al*., [22] studied a potential catalyst of WO_3/ZrO_2. The WO_3 was designated as 5, 10, 15, 19 and 25% on ZrO_2 and calcined at 700^oC. It can be seen that the BET specific surface area has a maximum at 5wt% of WO_3. It reveals the formation of a single, tetragonal phase of ZrO_2 up to 19wt% of WO_3 , whereas the WO_3/ZrO_2 sample with 25% of WO_3 shows tetragonal ZrO_2 and monoclinic WO_3. Ramu *et al*., [23] suggested that the ranging of 15-25% of W loadingsare found to be amorphous. When the hydrous zirconia is thermally treated the tratagonal crystallites grow and during cooling they get transformed into the thermodynamically stable monoclinic phase. Karim *et al*., and Chen *et al*., [24, 25] concluded that increasing the WO_3 loading led to a continuous decrease in peaks ascribed to monoclinic phase of ZrO_2 and an increase in the peak ascribed to the tetragonal phase. Kuba *et al*., and Kourieh *et al*., [17, 26] found that the WO_3 inhibits the sintering of ZrO_2 crystallites and the transformation to monoclinic ZrO_2 crystallites.

2.2 Boron and gallium on catalyst

Several studies have much attention to improve the textural properties of the materials normally giving high specific surface areas and pore sizes of zirconia. For example, the use of non-surfactant organic compounds, such as hydroxyacids and

urea, has been reported for the preparation of oxides using the sol-gel method [27]. The addition of boric acid and gallium to the zirconium oxide has not been much studied, though it may lead to materials with interesting acid characteristics.

Osiglio and Blanco [28] studied the effect of the addition of boric acid to zirconia synthesized employing pore-forming agents. In this work, zirconia was prepared employing the micelar method from zirconyl chloride as precursor, ammonium hydroxide as precipitating agent, final pH = 10, aging time of the hydrogel of 72 h, calcination of the samples at 320 ºC. The effect of the addition of glucose and polyethylene glycol (PEG) of different molecular weight in the characteristics of the obtained materials was studied. Boron was added to the zirconias employing an aqueous solution of boric acid by means of wet impregnation. The BET result shown the boric acid samples presented higher values of SBET . All the borated zirconias presented very strong acid sites. The XRD exhibited good dispersion on the surface of the hydrated oxide and that almost directly contribute to the acidity of the samples, because Bronsted acid sites can be generated by hydration of boron species, or the Lewis acidity of the zirconium ions can be increased by inductive effect.

Xu *et al*., [29] studied the effect of boron on the stability of Ni catalyst during steam methane reforming. Supported nickel catalysts were prepared by aqueous slurry impregnation using a nickel nitrate solution ($Ni(NO_3)_2 \cdot 6H_2O$ to produce Ni loadings of approximately 15 wt% on a commercial γ -Al_2O_3 and dried at 80 $^{\circ}$C in a rotor evaporator, kept overnight at 80 $^{\circ}$C in an oven, heated to 400 $^{\circ}$C with a 1°C/min ramp rate, and calcined in air at 400 $^{\circ}$C for 2 h. After calcination, boric acid (H_3BO_3, Sigma–Aldrich, 99% purity) was sequentially to produce boron loadings of approximately 0.5 and 1.0 wt%. The result shown that the promotion with 1.0 wt% boron increases the initial methane conversion from 56 to 61and reduce the first order dactivate rate , the unpromoted catalyst lost 21% of its initial activit while 0.5 wt% boron reduced from 21% to 14% and reduce to 6% with 1 wt% boron. It indicate that promotion with 1.0 wt% B improves the stability and the residual activity of a Ni catalyst.

TU *et al.*, [30] report effect of Ga_2O_3 on a $Pt/WO_3/ZrO_2$ Catalyst for *n*-Heptane Isomerization. The $Ga(OH)_3$-$Zr(OH)_4$ (Ga_3^+/Zr_4^+ atomic ratio = 0.02) was mixed under stirring of a 6 mol/L NH_4OH solution to a 0.2 mol/L aqueous solution of $ZrO(NO_3)_2$ containing $Ga(NO_3)_3$ to pH 9. The precipitate was then filtered, washed, and dried overnight. WO_3/Ga_2O_3-ZrO_2 (denoted WGZ) was prepared by incipient wetness impregnation of $Ga(OH)_3$-$Zr(OH)_4$ with an aqueous solution of ammonium metatungstate followed by drying and then calcination in static air at 800 ^oC for 3 h. The powder XRD patterns showed a mixture of the tetragonal and monoclinic phases of zirconia of Pt/WGZ and Pt/WZ. The Pt/WGZ catalyst exhibited stronger diffraction peaks characteristic of tetragonal ZrO_2 than Pt/WZ while weaker peaks attributed to monoclinic ZrO_2. the incorporation of small amounts of Ga_2O_3 into the Pt/WZ catalysthelped to stabilize the tetragonal phase of zirconia and inhibit the transformation from the metastable tetragonal phase to the monoclinic phase at the high calcination temperature. The Pt/WGZ catalyst gave a higher C7 isomerization selectivity at the same *n*-C7 conversion than Pt/WZ. For the acidity which measure by in situ FTIR spectroscopy. The incorporation of small amounts of Ga_2O_3 into WZ resulted in an increase in Bronsted acidity and ratio of Bronsted acidity to Lewis acidity.

Hwang and co worker [31] compared the promotion effects on sulfated mesoporous zirconia catalystsachieved by alumina and gallium. aluminum sulfate (AS/MP-ZrO_2) , gallium sulfate (GS/MP-ZrO_2), and ammonium sulfate was incipient wetness impregnation in the quantity of each source dissolved in 75% (vol.%) alcohol solution. The effects on surface area and pore sizes, the loadings of Al and Ga give similar results. For the acidity, they concluded that Al and Ga have been found not only to increase the total amount of surface acidic sites but also to change the balance of the types of surface acidity. The optimum amount of Al or Ga loading would give the optimum distribution of the type of acid sites.

Kaivalchatchawal *et al*., [32] studied the effect of Ga- and BCl_3-modified silica-supported. They prepared Ga by used $Ga(NO_3)_3$ source and impregnated onto silica gel with 0.2 wt.% of Ga. The resulting mixture was reffered to SiO_2–Ga. For the BCl_3 treated with that 14.25 g silica and added 150 ml for diluents , added 7 ml of BCl_3. The mixture was stirred for 30 min in an oil bath at 313 K, until temperature was raised up to 343 K, followed by drying under vacuum. The resulting mixture was referred to SiO_2–BCl_3.The BET surface area not different in SiO_2 support, SiO_2–Ga and SiO_2–BCl_3. The SiO_2 support exhibited no peak, indicating no acidic sites in temperature-programmed desorption of ammonia. However, determined desorption at 283 and 325 lmol NH_3/g on SiO_2–Ga and SiO_2–BCl_3 . That mean the acidity of silica support can be improved with the modification of Ga and BCl_3. The activities of ethylene/1-hexene copolymerization with silica-supported CGC/MAO catalyst can be improved with the Ga and BCl_3 acidic modification on the silica support.Increased activity was due to the stronger interaction between support and cocatalyst coupled with a formation of acidic sites derived from the modification. Additionally,BCl_3 is able to be a spacer on the silica support leading to the highest activity.

2.3 Precipitation Method

Chemical precipitation formation of a separable solid substance from a solution, either by converting the substance into an insoluble form or by changing the composition of the solvent to diminish the solubility of the substance in it. The distinction between precipitation and crystallization lies largely in whether emphasis is placed on the process by which the solubility is reduced or on that by which the structure of the solid substance becomes organized.

Precipitation often is used to remove metal ions from aqueous solutions: silver ions present in a solution of a soluble salt, such as silver nitrate, are precipitated by addition of chloride ions, provided, for example, by a solution of sodium chloride; the chloride ions and the silver ions combine to form silver chloride, a compound that is

not soluble in water. Similarly, barium ions are precipitated by sulfate ions, and calcium by oxalate; schemes have been developed for analysis of mixtures of metal ions by successive application of reagents that precipitate specific ions or groups of related ions

In many cases it is possible to select conditions under which a substance precipitates in highly pure and easily separable form. Isolation of such precipitates and determination of their weights constitute accurate methods for determining the amounts of various compounds.

Avila *et al.*, [33] investigate the feect produced on the structural characteristic of zirconia power by precipitation method. A 0.6M $ZrOCl_2.8H_2$ precipitated with 6M NH_4OH_4 / 4 M NaOH and control pH at value of 6, 10.4 and 13.5. At pH 13.5, they varied 2 condition as held the NaOH solution at 40^oC and kept at room temperature. Thermogravimetric result show that the mass loss up to 200^oC. The total mass loss up to 20% in PH 10.4 and 13.5, in pH 6 the mass loss up to 24.5%. Due to increase the structure bound content with decrease PH. The diffractogram profile after calcination exhibited a mixture of monoclinic and tetragonal reflections. The crystallite size at pH 6 and 10.4 exhibited the m reflection are slightly higher than the t reflection. For the pH 10 at room temperature, the crystallite size are hundred percent tetragonal.

Wang *et al.*, [34] studied by compared the nanocrystalline zirconia prepared by precipitation and sol–gel methods. Precipitation method prepared by used zirconyl chloride ($ZrOCl_2 \cdot 8H_2O$) 13.07 g of zirconyl chloride ($ZrOCl_2 \cdot 8H_2O$) in 500 ml of water was dropped into a recipient containing 300 ml of water. While the solution was stirred, a solution of 0.1M ammonia was dropwise added to it until reaching pH 10. This alkaline solution was continuously stirred for 1 h, and then aged for 24 h until forming a precipitate, which was washed several times with distilled water. The precipitate was dried at $120^{\circ}C$ for 4 h to obtain the fresh sample. For the sol-gel method prepared by Zirconium *n*-butoxide (11 ml) dissolved into35.2 ml of absolute ethanol under continuous stirring. The homogeneous solution was dropped in to the hydrolysis catalyst (NH_4OH) until reaching pH 10.Thereafter, 2 ml of water were

dropped, and the new solution was stirred continuously until gelling. The gel was dried at room temperature in a vacuum for 24 h..They varied calcined temperature 400 600 and 800^{o}C. Both synthesis methods gave rise to nanocrystalline zirconia.

2.4 Solvothermal Method

The hydrothermal or solvothermal [35] technique has become one of the most important methods for the fabrication of nanostructural materials. In recent years, a tremendous number of nanomaterials have been processed by hydrothermal or solvothermal method and thousands of science papers about the hydrothermal/ solvothermal synthesis of nanomaterials have been published. From the perspective of morphology of nanomaterials, the hydrothermal technique has been used to process nanomaterials with a variety of morphological features, such as nanoparticle, nanosphere, nanotube, nanorod, nanowire, nanobelt, nanoplate, and so on. From the perspective of composition of nanomaterials, the hydrothermal technique can be used to process almost all types of advanced materials. The hydrothermal or solvothermal technique is not only used to process simplest nanomaterials,but also acts as one of the most attractive techniques for processing nanohybrid and nanocomposite materials. In short words, the great advantages of hydrothermal technology for nanomaterials processing are the production of particles that are monodispersed with total control over their shape and size in addition to their chemical homogeneity with the highest dispersibility.

Solvothermal processes [36] refer to chemical reactions that are performed in a closed reaction vessel at temperatures higher than the boiling point of the solvent employed. Solvothermal processes are mainly defined by chemical parameters such as the nature of the reagents and of the solvents, and by thermodynamical factors, in particular temperature and pressure. Although solvothermal techniques have a long history, for a long time their whole focus was on the processing of bulk crystals and bulk materials, and fine grained powders, often obtained by these approaches, were discarded due to the lack of suitable characterization tools. With the growing interest in sub-micron and nanosized powders with well-defined sizes and morphologies,

solvothermal syntheses became a fundamental branch of nanoparticle preparation and processing. The trend towards greener technologies further strengthens these approaches, because on the one hand they consume less energy, due to the moderate reaction temperatures, and on the other hand they allow the use of common, inexpensive laboratory solvents, whose low boiling points constituted the main limitation for nanoparticle synthesis]. More information about hydro- and solvothermal processes including equipment and technical details can be found somewhere else .Examples of metal oxide nanoparticles prepared under solvothermal conditions and in the presence of surfactants are magnetite, ceria, hematite, tin oxide cobalt oxides or ZnO, N-doped ZnO and CdO.

Li *et al*., [37] studied the phase composition controllable preparation of zirconia nanocrystals via solvothermal method. They prepared Zr by dissolving $ZrOCl_2.8H_2O$ into ethyl alcohol and fixed concentration of 0.2M. The gel precursor was adding 1.25M KOH ethanol solution. They varied reaction time range 0 to 60 min at 180^oC and washed with deionized water to remove the soluble chlorides and ethanol to depress agglomeration and dried in vacuum dry in chamber at 85^oC for 5 h. Phase composition of particles was determined by XRD measurement using CuKα as radiation source. The result shown no marked differences on crystallite size of m-ZrO_2 among all sample, while the content and crystallite size of m-ZrO_2 increase with the progressing of solvothermal. By Crystallite size estimated from XRD patterns using Scherrer equation shows that the t-ZrO_2 is below 5 nm, while the size of the m-ZrO_2 varies from 10 nm to 50 nm.

Uchiyama *et al*., [38] studied the Solvothermal synthesis of size-controlled ZrO_2 microspheres via hydrolysis of alkoxides modified with acetylacetone. They address the synthesis of size-controlled ZrO_2microspheres from the solutions containing $Zr(OC_3H_7\ n)_4$, H_2O, n-C_3H_7OH and acac (acetylacetone) via solvothermal process.They varied a molar composition of the precursor solutions ($Zr(OC_3H_7\ n)_4$) X= 50–200 , the amounts of H_2O (y = 0.5-4) , n-C_3H_7OH (Z = 0-10) and acac in the solutions. It can be concluded that the increase in the amount of n-C_3H_7OH and H_2O at a constant n-C_3H_7OH/H_2O mole ratio could provide the moderate increase in the

hydrolysis and nucleation rates, and consequently decrease the size of the ZrO_2 spheres. Although the hydrolysis of alkoxides is accelerated by an increase in the amount of H_2O in the solution, the much larger amount of H_2O also lead to the rapid formation of unshaped particles or the gelation of the precursor solutions. However, the increase in the amount of alcoholic solvents decreases the hydrolysis rate, and consequently suppresses the rapid precipitation and the gelation. Spherical particles of 0.5–2 nm in diameter were found ZrO_2 products

Niedrberger and coworker [36] reported a widely applicable solvothermal route to nanocrystalline iron, indium, gallium and zinc oxides base on the reaction between the corresponding metal acetylacetonate as metal oxide precursor and benzylamine as solvent .They proved that with the exception of the iron oxide system, in which a mixture of the phase magnetite and maghemite is formed, only phase pure materials are obtained, γ-Ga_2O_3, zincite ZnO and cubic In_2O_3. The particle sizes lie in ranges 15-20 nm for the iron, 10-15 nm for the idium, 2.5-3.5 nm for the gallium and around 20 nm for the zinc oxide, Moreover, the same group developed mixed nanocrystalline $BaTiO_3$, $SrTiO_3$, and (Ba, Sr)TiO_3.$BaTiO_3$ nanoparticles are nearly spherical in shape, while $SrTiO_3$ particles display less-uniform particle shapes, the size varying between 5 and 10 nm.

Chapter III

Theory

3.1 Esterification

Esterification [39] is a chemical reaction in which two reactant, an alcohol and an acid, form an ester as the final reaction product. It is a reversible reaction, as a result of reversibility, many esterification reactions are equilibrium reactions.

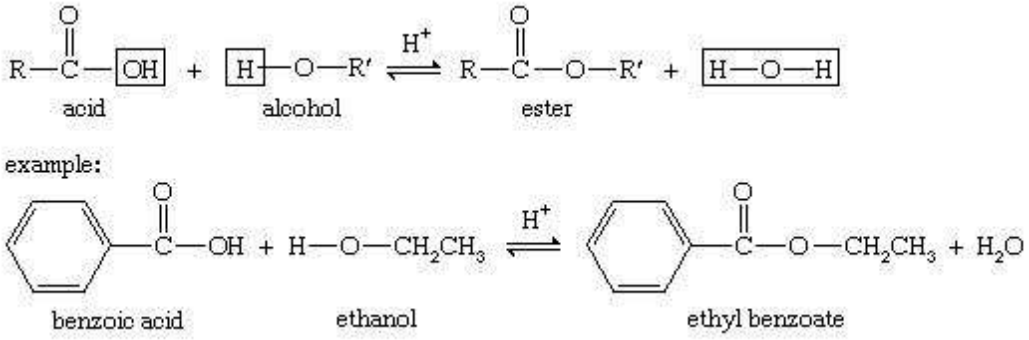

Figure 3.1.1 Carboxylic acid esterification.

The mechanism of homogeneous catalyzed esterification has long been established. Because the reaction is reversible, an equilibrium mixture is produced containing all four of the substances in the equation. In order to get the forward reaction, the formation of esters from carboxylic acids and alcohols in the presence of concentrated sulphuric acid acting as the catalyst. It uses the formation of ethyl ethanoate from ethanoic acid and ethanol as a typical example.

Figure 3.1.2 The formation of esters from carboxylic acids and alcohols.

Step 1

In the first step, the ethanoic acid takes a proton (a hydrogen ion) from the concentrated sulphuric acid. The proton becomes attached to one of the lone pairs on the oxygen which is double-bonded to the carbon.

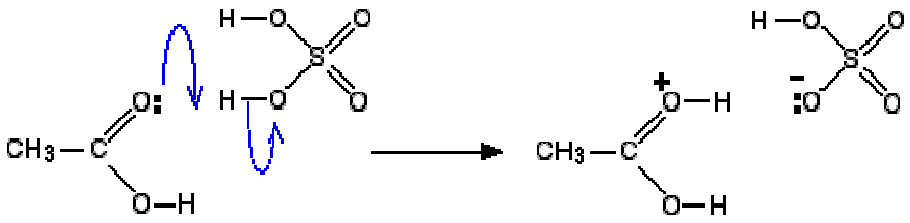

Figure 3.1.3 The ethanoic acid takes a proton.

The transfer of the proton to the oxygen gives it a positive charge. The positive charge is delocalized over the whole of the right-hand end of the ion, with a fair amount of positiveness on the carbon atom.

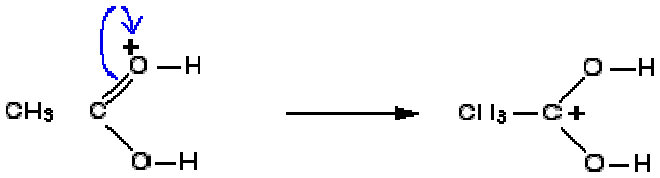

Figure 3.1.4 The proton transfer to the oxygen.

Which can written the delocalized structure of the ion in these form.

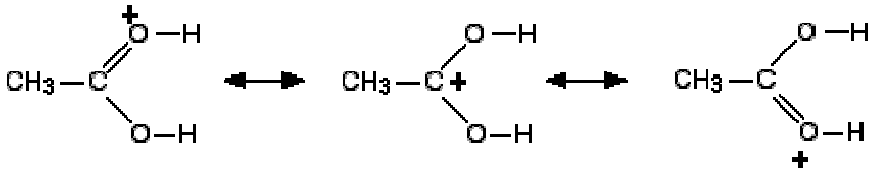

Figure 3.1.5 The several delocalized structure.

Step 2

The positive charge on the carbon atom is attacked by one of the lone pairs on the oxygen of the ethanol molecule.

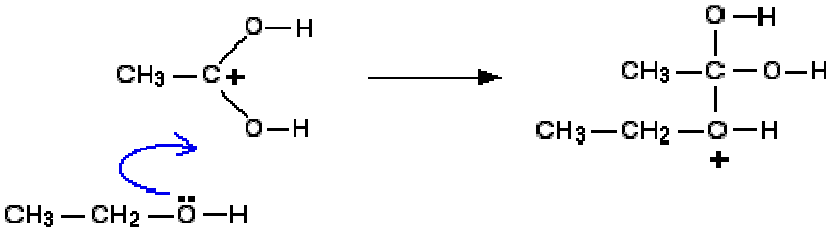

Figure 3.1.6 The positive charge on the carbon.

Step 3

A proton (a hydrogen ion) gets transferred from the bottom oxygen atom to one of the others. It gets picked off by one of the other substances in the mixture (for example, by attaching to a lone pair on an unreacted ethanol molecule), and then dumped back onto one of the oxygen more or less at random. The net effect is.

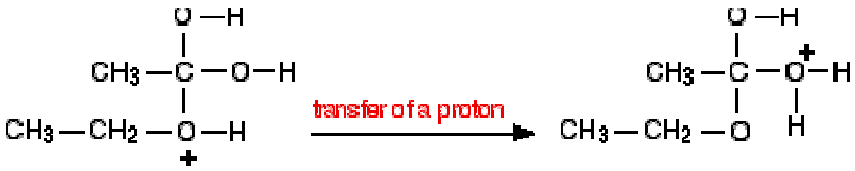

Figure 3.1.7 Transfer of a proton.

Step 4

A molecule of water is lost from the ion.

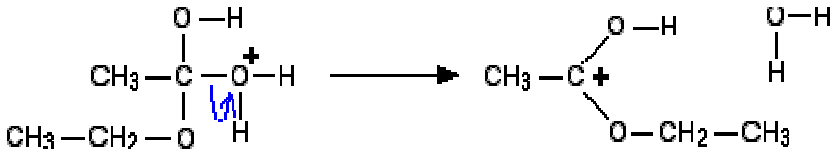

Figure 3.1.8 A molecule of water is lost from ion.

Step 5

The hydrogen is removed from the oxygen by reaction with the hydrogen sulphate ion which was formed way back in the first step.

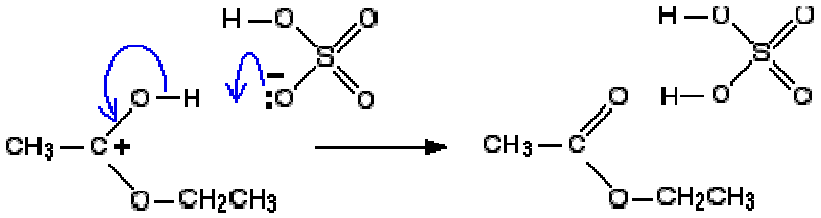

Figure 3.1.9 Final mechanism of esterification reaction.

The ester has been formed, and the sulphuric acid catalyst has been regenerated. For reverse reaction, at the mechanism for the hydrolysis of ester in the presence of a dilute acid

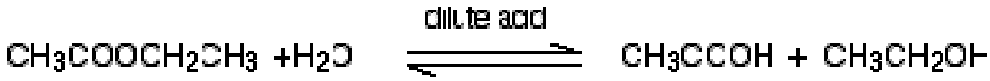

Figure 3.1.10 the hydrolysis of esters in the presence of a dilute acid.

Step 1

The actual catalyst in this case is the hydroxonium ion, H_3O^+, present in all solutions of acids in water. In the first step, the ester takes a proton (a hydrogen ion) from the hydroxonium ion. The proton becomes attached to one of the lone pairs on the oxygen which is double-bonded to the carbon.

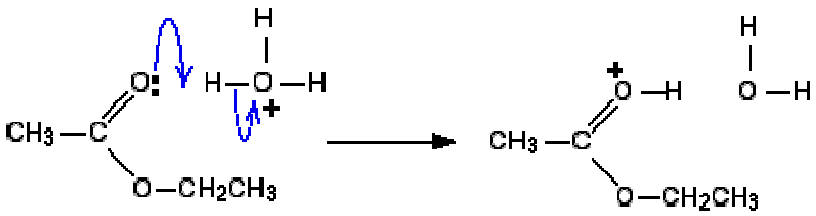

Figure 3.1.11 The ester takes a proton from the hydroxonium ion.

The transfer of the proton to the oxygen gives it a positive charge, but the charge is actually delocalized (spread around) much more widely than this shows.

Step 2

The positive charge on the carbon atom is attacked by one of the lone pairs on the oxygen of a water molecule.

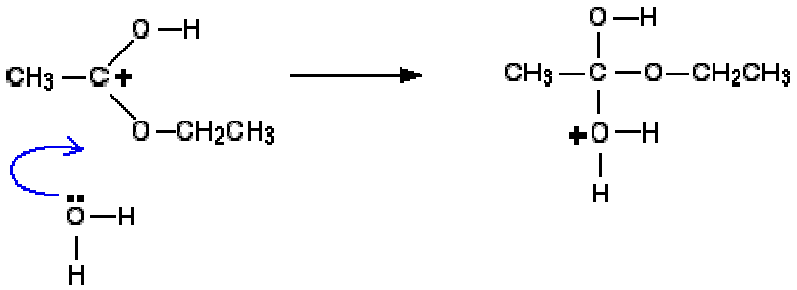

Figure 3.1.12 The carbon atom is attacked by one of the lone pairs on the oxygen.

Step 3

A proton (a hydrogen ion) gets transferred from the bottom oxygen atom to one of the others. It gets picked off by one of the other substances in the mixture (for example, by attaching to a lone pair on a water molecule), and then dumped back onto one of the oxygen more or less at random.

Eventually, by chance, it will join to the oxygen with the ethyl group attached. When that happens, the net effect is:

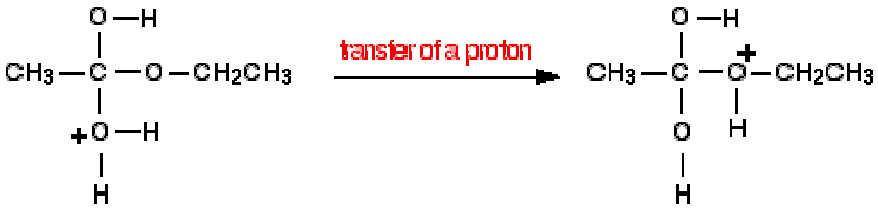

Figure 3.1.13 A proton transfer from bottom oxygen to one of the others.

Step 4

Now a molecule of ethanol is lost from the ion. That is one of the products of the reaction

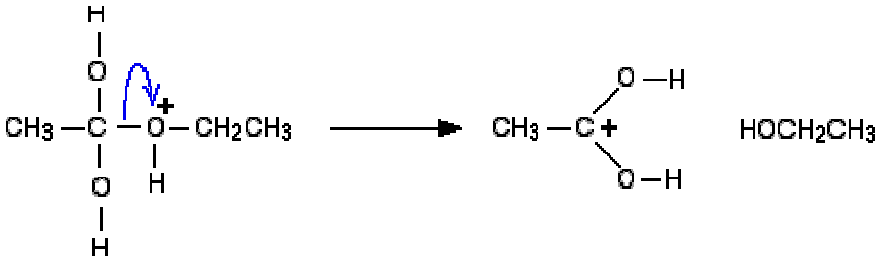

Figure 3.1.14 A molecule of ethanol is lost from the ion.

Step 5

The hydrogen is removed from the oxygen by reaction with a water molecule.

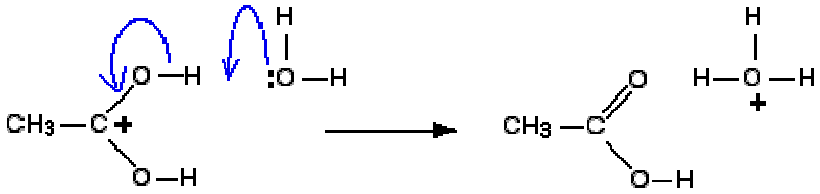

Figure 3.1.15 The hydrogen is removed from the oxygen.

Then, the ethanoic acid (the other product of the reaction) and the hydroxonium ion catalyst has been regenerated.

3.2 Solid Acid catalyst

Solid Acid catalysis [40] is employed in a large number of industrial reactions, among them the conversion of petroleum hydrocarbon to gasoline and related products. Such reactions include decomposition of high-molecular-weight hydrocarbons (cracking) using alumina–silica catalysts (Bronsted–Lowry acids), polymerization of unsaturated hydrocarbons using sulfuric acid or hydrogen fluoride (Bronsted–Lowry acids), and isomerization of aliphatic hydrocarbons using aluminum chloride (a Lewis acid). Solid-acid catalysts are generally categorized by their

Bronsted and/or Lewis acidity, the strength and number of these sites, and the morphology of the support (e.g., suface area, pore size). The synthesis of pure Bronsted and pure Lewis acid catalysts attracts a great degree of academic interest, although the latter is harder to achieve because Bronsted acidity often arises from Lewis acid-base complexation, as illustrated in **Figure 3.2.1**

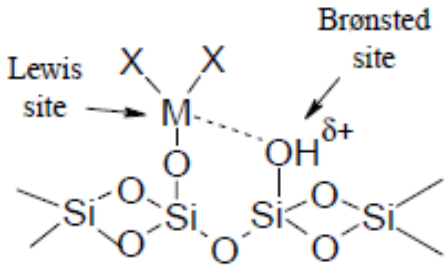

Figure 3.2.1 Bronsted acidity arising from inductive effect of Lewis acid center coordinated to a silica support.

Preparations of Solid Acid Catalysts compounds are made by grafting acid catalytic sites on polymer surfaces. The polymers should be insoluble in the solvent medium, and should have a large surface area in order to accommodate as many catalytic sites as possible. The mechanical strength of a given polymer matrix (also called the 'support') limits the temperature at which a given reaction can be carried out. If the polymeric matrix starts disintegrating at, say, 135^{o}C, the reaction obviously has to be carried out below this temperature. Initially, the polymeric surfaces used were of natural origin (e.g.the 'clay minerals'), but in recent times, they are tailor-made for specific reactions. For example, chemically modified alumina, silica, zeolites and synthetic resins are used as supports.

Clay minerals

Clays were the first solid acid catalysts used in organic synthesis. However, due to their wide variety they lack perfect reproducibility in yields with different samples. Otherwise, they have considerable potential as environmental friendly solid

acid catalysts. Some of the types of clays frequently used are Bentonite, Montmorillonite K10 and Montmorillonite-KSF.

Amorphous Silicas and Aluminas

Silica and alumina constitute a group of polymeric oxides of silicon and aluminium respectively. They can also be obtained in mixed polymeric forms. Their anhydrous forms have a general structure as shown in **Figure 3.2.2** On hydration, some divalent oxide linkages are replaced by M-OH bonds in the matrix . The protons released on ionization of these O-H bonds are the source of Bronsted acidity .Oxides like titania, zirconia, magnesia as well as mixed oxides are also used. The physical structures of all these oxides consist of random pores in which adsorption and catalysis takes place. Hence the surface is very irregular. The extent of their usefulness is dependent on particle size, surface area, pore structure and acidity. For instance, the surface area of silicas should be in the range of 50 – 400 m^2/g and that of aluminas should be in the range of 120 – 300 m^2/g

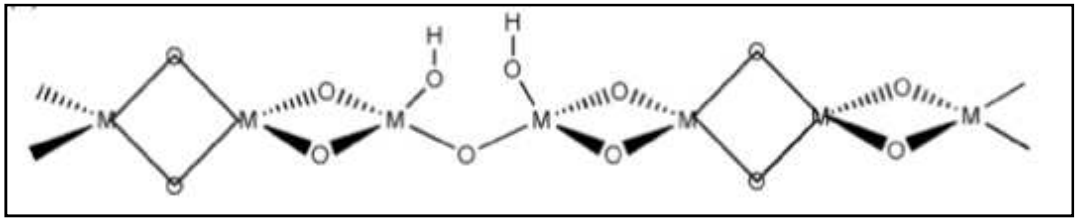

Figure 3.2.2 Representative structure of hydrated silica and alumina.

Zeolites

Zeolites are also known as molecular sieves. They are aluminosilicates with the general formula $Na_x[(AlO2)_x(SiO2)_y][H2O]_y$. They have a tetrahedral structure with each atom of silicon and aluminium surrounded by oxygen atoms as **Figure 3.2.3.** In natural samples, they have three-dimensional crystalline microporous channels in which molecules of appropriate size can diffuse and react. The pore size in zeolites can be controlled using synthetic methods. In the three-dimensional

structure illustrated in **Figure 3.2.4**, it can be seen that the four-bonded tetravalent silicon site is neutral whereas the four-bonded trivalent aluminium site is negative.

This requires positively charged counter-ions such as Na^+, as indicated in the general formula for zeolites.

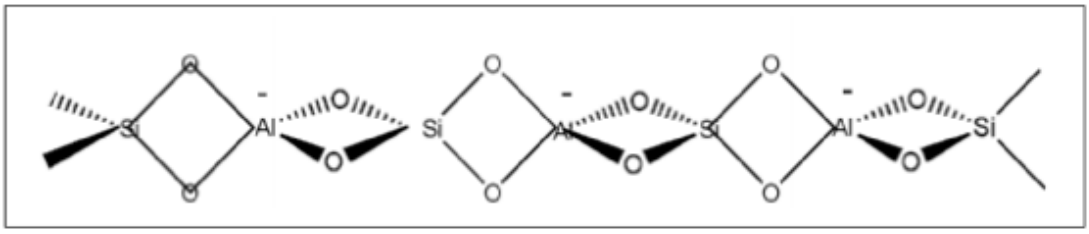

Figure 3.2.3 Representative structure of the zeolite skeleton.

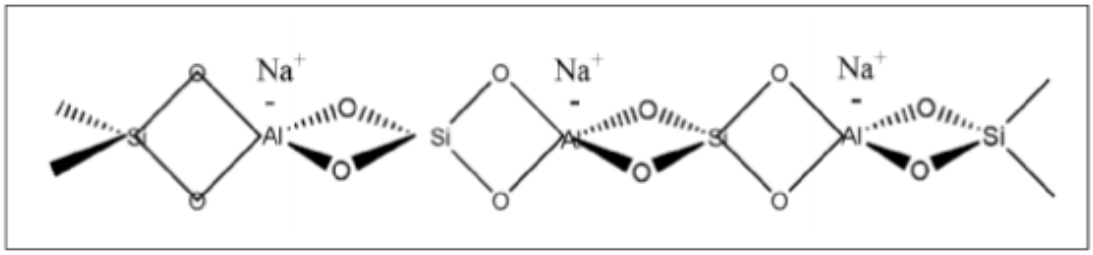

Figure 3.2.4 Representative structure of zeolite.

In order to make the zeolite acidic, sodium counter-ions are replaced with protons. This is done by first exchanging the sodium ions with ammonium ions (Figure 3.2.5) and then heating the zeolite sample. On heating, NH_3 is released and protons are left behind as the counter-ions, in place of sodium ions (Figure 3.2.6). So each aluminum ion will have a proton counter-ion in the zeolite network and this is the cause of its Bronsted acidity. In other words, the ratio Si/Al determines the polarity, the acidity

3.3 Bronsted and Lewis

In 1923, British chemists Johannes Nicolaus Bronsted and Thomas Martin Lowry independently developed definitions of acids and bases based on the compounds' abilities to either donate or accept protons (H^+ ions). In this theory, acids are defined as proton donors; whereas bases are defined as proton acceptors. A compound that acts as both a Bronsted-Lowry acid and base together is called amphoteric [41].

Bronsted - Lowry theory states that:
An acid produces protons (H^+ ions) and donates them to a base, which accepts it.
Therefore an acid is a proton donor and a base is a proton acceptor.

Acids and bases co-exist together as conjugate pairs.
Acid-base conjugate pairs are linked by a proton (H^+)

$$\underset{\text{base}}{NH_{3(g)}} + \underset{\text{acid}}{H_2O_{(l)}} \leftrightarrow \underset{\text{acid}}{NH_4^{+}{}_{(aq)}} + \underset{\text{base}}{OH^-}$$

- NH_3 is a base because it accepts a proton from H_2O. When the proton is accepted it becomes the conjugate acid NH_4^+
- NH_4^+ is a conjugate acid because it is capable of donating a proton to form NH_3.
- NH_3 and NH_4^+ are conjugate acid-base pairs.
- H_2O is an acid because it donates a proton becoming the conjugate base, OH^-.As a (conjugate) base, OH^- can accept a proton to form H_2O.
- H_2O and OH^- are called conjugate acid-base pairs.

Bronsted-Lowry theory can also be used to explain the dissociation or ionization of water. In B-L theory water dissociates when it reacts with itself. One water molecule acts as an acid because it accepts a proton, H^+ from the other water molecule which acts as a proton acceptor or base to form H_3O^+ and OH^-

$$H_2O_{(l)} + H_2O\ (l) \leftrightarrow H_3O^+(aq) + OH^-\ (aq)$$
acid base conj acid conj base

NOTE: The term 'amphoteric' is also used to describe a substance that can act as both acid and base. We used amphoteric to describe how aluminum oxide can act as both an acid and a base.

Acting as a base $Al_2O_{3(s)} + 6\ HCl_{(aq)} \rightarrow 2\ AlCl_{3(aq)} + 3\ H_2O_{(l)}$

Acting as a acid $Al_2O_{3(s)} + 2\ NaOH_{(aq)} + 3\ H_2O_{(l)} \rightarrow 2NaAl(OH)_{4(aq)}$

In Bronsted and Lowry theory:

Monoprotic is the name given to an acid or base that donates or accepts one proton. Diproticis the name given to an acid or base that donates or accepts two protons. Polyprotic is the name given to an acid or base that donates or accepts more than one proton.

Strength of B-L Acid-Base Conjugate Pairs

Generally: Strong acids have weak conjugate bases

Weak acids have strong conjugate bases

Lewis Theory

In Lewis theory bases are species with a non bonding pair of electrons which they donate to and acid. The bond formed between the acid and base is a coordinate covalent bond.

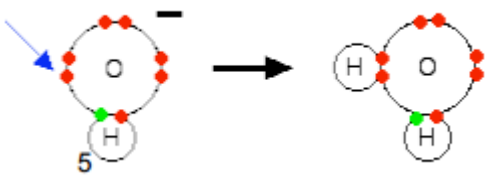

$$H^+ + OH^- \leftrightarrow H_2O$$

Figure 3.3.1 The bond formed between the acid and base is a coordinate covalent bon

A non-bonding pair of electrons on the oxygen atom (shown by the arrow) of the hydroxide ion is donated to hydrogen ion. Circle the coordinate bond in water. A coordinate bond (or dative bond) is a covalent bond where one species provides the lone pair of electrons for the other species accepts it. It is different from a normal covalent bond where both atoms contribute an equal number of electrons to the bond.

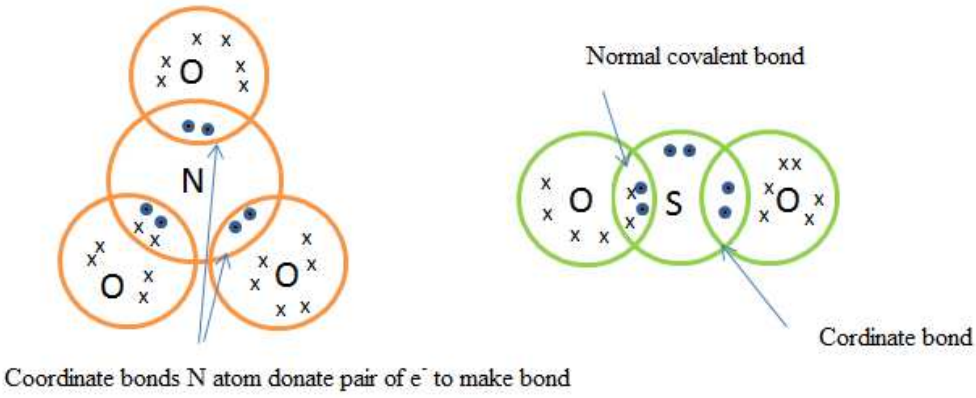

Figure 3.3.2 The bond formed between the acid and base is a coordinate covalent bond.

Lewis's theory complements Bronsted-Lowry theory by extending the range of acids and bases to include those that do not involved hydrogen or protons at all like the boron trifluroide molecule, BF_3.

In the Lewis acid base reaction between a proton and ammonia the non-bonding pair of electrons on the nitrogen atom (shown by the arrow) of the ammonia is donated to the hydrogen ion.

$$H^+ \quad + \quad NH_3 \quad \leftrightarrow \quad NH_4^+$$

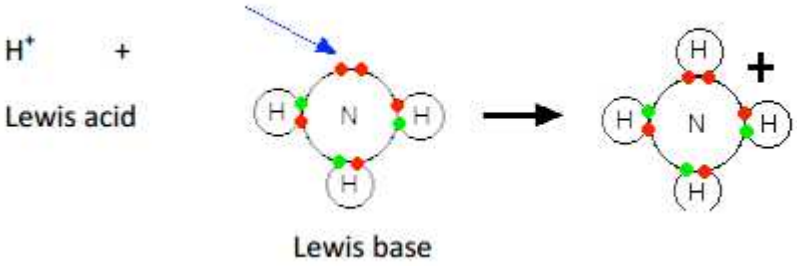

Figure 3.3.3 The ammonia is donated to the hydrogen ion.

Circle the coordinate bond in the ammonium ion

When ammonia (lewis base) reacts with hydrogen chloride (lewis acid), in the mechanism the curly arrows show the movement of the pairs of electrons.

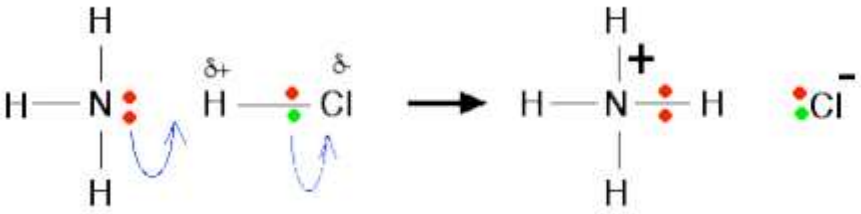

Figure 3.3.4 The ammonia react with hydrogen chloride

Chapter IV

Experimental

The research scope and methodology were described in this chapter which consisted of material and chemicals, catalyst preparation, catalyst characterization and reaction study in esterification.

4.1 Research Methodology

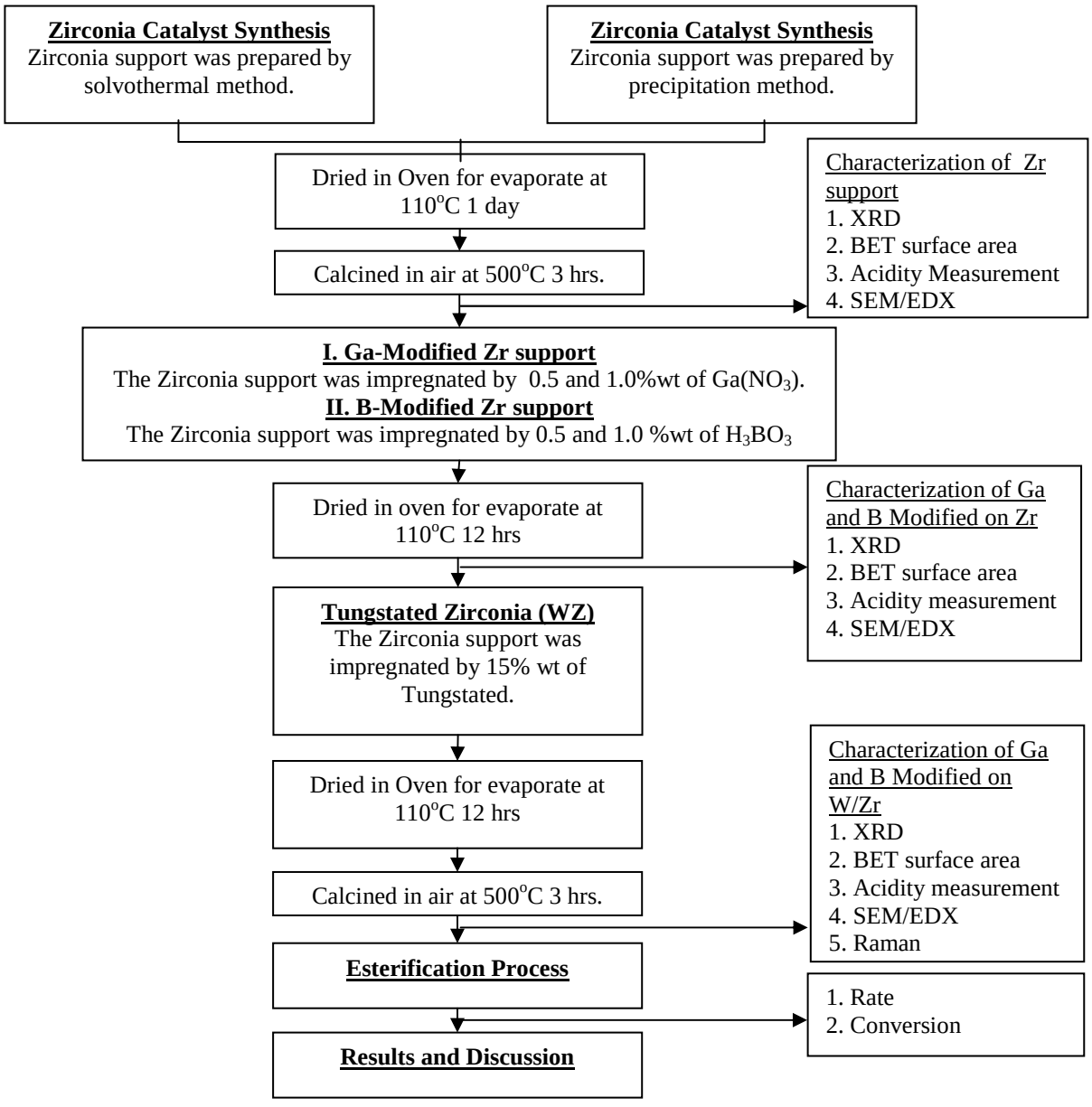

Figure 4.1 Research Methodology

4.2 Preparation catalyst

4.2.1 Material and Chemical

1. Zirconium n-butoxide (97%, Aldrich)
2. 1, 4-butanediol (99%, Sigma-Aldrich)
3. Methanol (99%, Sigma-Aldrich)
4. Zirconyl nitrate Hydrate (99.9%, Aldrich)
5. Ammonium Hydroxide (Sigma-Aldrich)
6. Boric acid (Sigma-Aldrich)
7. Gallium(III) nitrate hydrate (99.9%,Aldrich)
8. Tungsten(VI) chloride (99.9%, Aldrich)

4.2.2 Preparation of ZrO_2 by solvothermal method

The nanocrystal zirconia were prepared by the solvothermal method described by Kongwudthiti *et al*.,[42].

Zirconium n-butoxide (97%, Aldrich) 30 g were suspended in 100ml of 1, 4-butanediol (99%, Sigma-Aldrich) in a test tube which was placed in 300 ml autoclave.Then, the 30ml of 1, 4-butanediol were added in the gap between the test tube and the auto clave. The autoclave was purged with nitrogen then it was heated to 300^{o}C with the rate of 2.5 ^{o}C/min and hold steadily 2 hrs. During the reaction, the autogeneous pressure gradually increased when the temperature raise cool down the autoclave to room temperature, The resulting product were repeatedly washed with methanol by vigorous mixing and centrifuging. then, dried in oven at 110^{o}C for 1 day and calcined at 500^{o}C for 3 hrs.

4.2.3 Preparation of ZrO_2 by precipitation method

Zirconyl nitrate [$ZrO(NO_3)_2$] (0.15M) was carried out by slowly adding a solution into a well-stirred precipitation solution of ammonia hydroxide (NH_4OH) (2.5wt%) at room temperature. The pH of the solution was carefully controlled at 10. The resulting precipitate was removed, and then washed with deionized water. The obtained sample was dried at 110^oC for 1 day and calcined at 500^oC for 3 hrs.

4.2.4 Preparation Ga and B modified on Zr support

The Ga and B source in the present is $Ga(NO_3)$ and H_3BO_3 . It was impregnated on to zirconia by either 0.5 and 1.0%wt of Ga or B. The support was dried in oven at 110^oC for 12 hrs.

4.2.5 Preparation Tungstated Zirconia (WZ)

The tungstated zirconia (W/ZrO_2) catalysts were prepared by the incipient wetness impregnation of modified zirconia obtained above.

The tungsten chloride was used in 15%wt of W and loaded in the sample. The catalyst was dried in oven at 110^oC for 24 hrs. and calcined in air at 500^oC for 3 hrs.

4.3 Catalyst Characterization Technique

The characteristic of catalyst were determined by the various characterization techniques as follows:.

4.3.1 X-Ray Diffraction (XRD)

Monochromatic powder X-Ray diffractograms was recorded in the 20-80^o 2θ range using a XDS 2001 (Scintag Inc.) instrument with Cu K_α radiation (λ = 1.54Å wavelength) for commercially available catalyst namely WZ. The preparation catalyst namely GA-WZ and B-WZ were collected with a SIEMEMS XRD D5000 using CuK_α radiation with a scan rate of 0.004^o(2θ) per second from 2θ = 10^o to 80^o

4.3.2 Scanning Electron Microscope (SEM)

Scanning Electron Microscope (SEM) was observed the surface morphology of the samples with an acceleration voltage of 15kV on Hitachi S-3400N. Gold was be coated on the samples to scaning.

4.3.3 N2 physic sorption (BET surface area)

Surface area of the samples was determined by using a multipoint BET method. Before this analysis, the catalyst was degassed at 300^{o}C and 10^{-3} mmHg for 3h. Adsorption measurement was carried out using liquid nitrogen at -196^{o}C in a Micrometrics ASAP 2020 device. The surface densities expressed as the number of atoms per nanometer square area was calculated using the equation as mentioned as follow

$$\text{Surface density} = \frac{[\text{Promoter loading}(\%)/100] \times 6.023 \times 10^{23}}{\text{Formular weight of promoter} \times \text{BET surface area } (m^2 g^{-1}) \times 10^{18}}$$

4.3.4 Acidity measurement

The number of acid sites were also estimated by using a method involving an aqueous ion-exchange step, in which 0.2 g of catalyst was added to 10 ml of a 3.42 M aqueous solution of NaCl under stirring. The exchange ions between H+ of catalyst and Na+ in the solution were carried out for 30 h at room temperature. The liquid was filtered off and titrated with a 0.05 N aqueous NaOH solution.

4.3.5 Raman Spectroscopy

The molecular structure of the supported tungsten oxide phase was determined using Raman spectroscopy since this technique has the ability to discriminate between the difference the tungsten oxide molecular structures. The Raman spectra of the samples were recorded using a Perkin Elmer Spectrum GX spectrometer, collected by projecting a continuous wave YAG laser of Nd (810nm) through the samples at room temperature. A scaning range of 700-1400 cm^{-1} with a resolution of $2cm^{-1}$ was applie.

4.4 Esterification Process

The modified tungstated/Zirconia catalysts were operated with esterification of acetic acid and methanol.

20 g of acetic (99.9% for concentrate acetic acid or 6M acetic acid for dilute acetic acid) and 2 wt% (on a concentrate acetic basis) of tunstated Zirconia catalyst were added in a closed 250ml regular glass reactor. The reaction was conducted at $60^{o}C$ with magnetic stirring and adds the methanol (3 eq. molar) to the mixture. The sample was withdrawn periodically from the reactor, quenched to room temperature. Then, separate the solid catalyst from product by centrifuged for prevent further reaction.

Determine the concentration of reacted sample by using a SHIMADZU gas chromotograph (GC-14B) equip with Chrompack SE52 column and flame ionization detector.

The reaction was repeated at different reaction times in order to obtain the acetic conversion profile. The acetic acid conversion(%) calculated as follows

$$\% \text{ Acetic acid conversion } = \frac{\text{initial acetic acid conc.} - \text{acetic acid conc at time}}{\text{initial actic acid conc}} \text{x}100$$

CHAPTER V

RESULT AND DISCUSSTION

In this chapter, the result and discussion are divided into three sections. Section 5.1 explains the characteristics of zirconia support with a comparison for the preparation method of solvothermal and precipitation. Section 5.2 explains the characteristics of Gallium modified ZrO_2 support for tungstated zirconia catalyst and the characteristics of boron modified ZrO_2 support for tungstated zirconia catalyst are explained in Section 5.3 respectively.

5.1 Characteristics of ZrO_2 and W/ZrO_2 catalyst for preparation method of solvothermal and precipitation

The color of zirconias prepared from the solvothemal and precipitation method are white after dried. **Figure 5.1- 5.2** show SEM image of the products under the preparation method. It was found that the samples prepared by the solvothermal method have a spherical shape and a dense mass. It appeared the secondary particles formed by aggregation of primary particles. Kongwudthitu *et al*., [42] proposed that the mechanism during crystallization of zirconia in the different glycols was completely different. In precipitation method, the samples were irregular and roughness shaped particles.

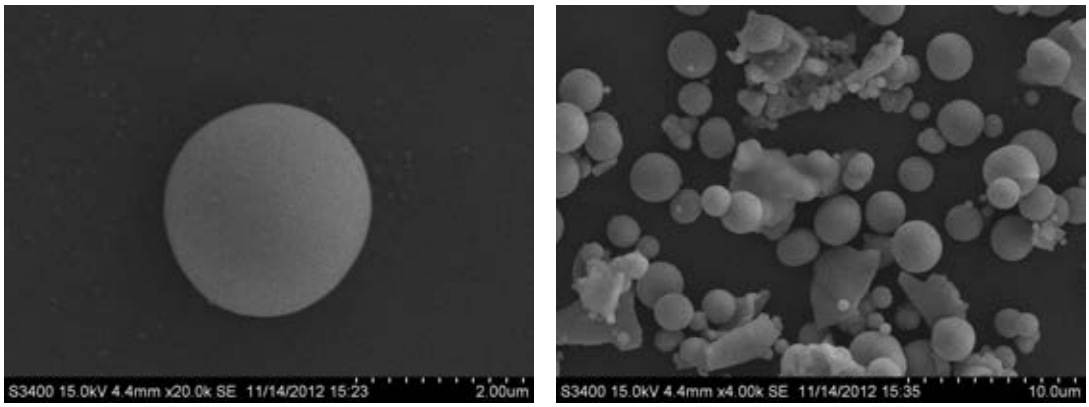

Figure 5.1 SEM micrograph of solvothermal Method

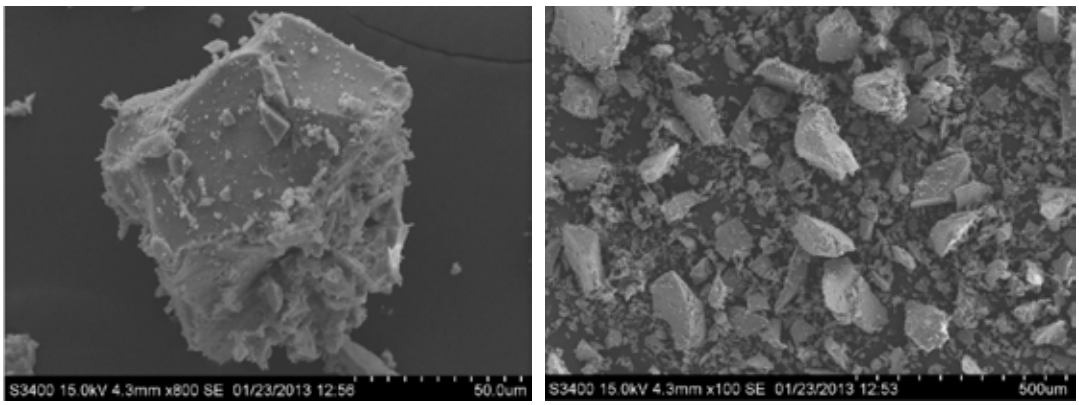

Figure 5.2 SEM micrograph of Precipitation Method

The X-ray diffraction patterns of the zirconia powders prepared by the solvothermal and precipitation are shown in **Figure 5.3** The XRD patterns indicate tetragonal crystalline zirconia (t-ZrO_2) at 30.2^o, 35.3^o and 50.6^o and monoclinic phase peaks at 24.3^o, 28.3^o and 31.4^o for both preparation products. The average crystallite size calculated from the XRD line broadening using the Scherrer equation and the BET surface areas of the zirconia are reported in **Table 5.1** The average crystallite size of both tetragonal and monoclinic phases in the precipitated sample were much less than that in solvothermal samples. On the other hand, the BET surface areas of precipitated sample were much large that of the solvothermal samples.

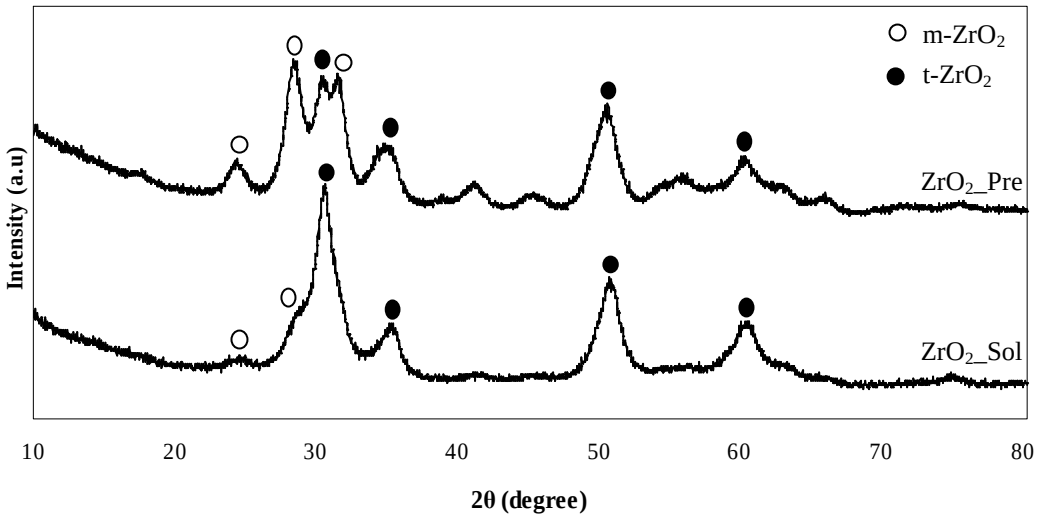

Figure 5.3 XRD patterns of the ZrO_2 prepared by the solvothemal and precipitation

Table5.1 Texural characterization of zirconia support

Sample	BET surface area (cm^3/g)	Crystallite Size [a] (nm)	Surface acidity [b] (µmol/g)	XRD Phase
ZrO_2_ Sol	150.89	3.5	45	m-ZrO_2, t-ZrO_2
ZrO_2_Pre	189.04	1.3	39	m-ZrO_2, t-ZrO_2

[a] Calculate of crystallite size by Debye-Scherrer equation

[b] Measured by Ion-Exchange and titration with 0.05N NaOH

The SEM/EDX micrograph of tungstated zirconia catalyst are shown in **Figure 5.4**. The support zirconia was impregnated with 15wt% of tungsten and calcined in air at 500°C for 3 h. The result exhibited that W was good distributed on the zirconia support and without any change in the zirconia morphology.

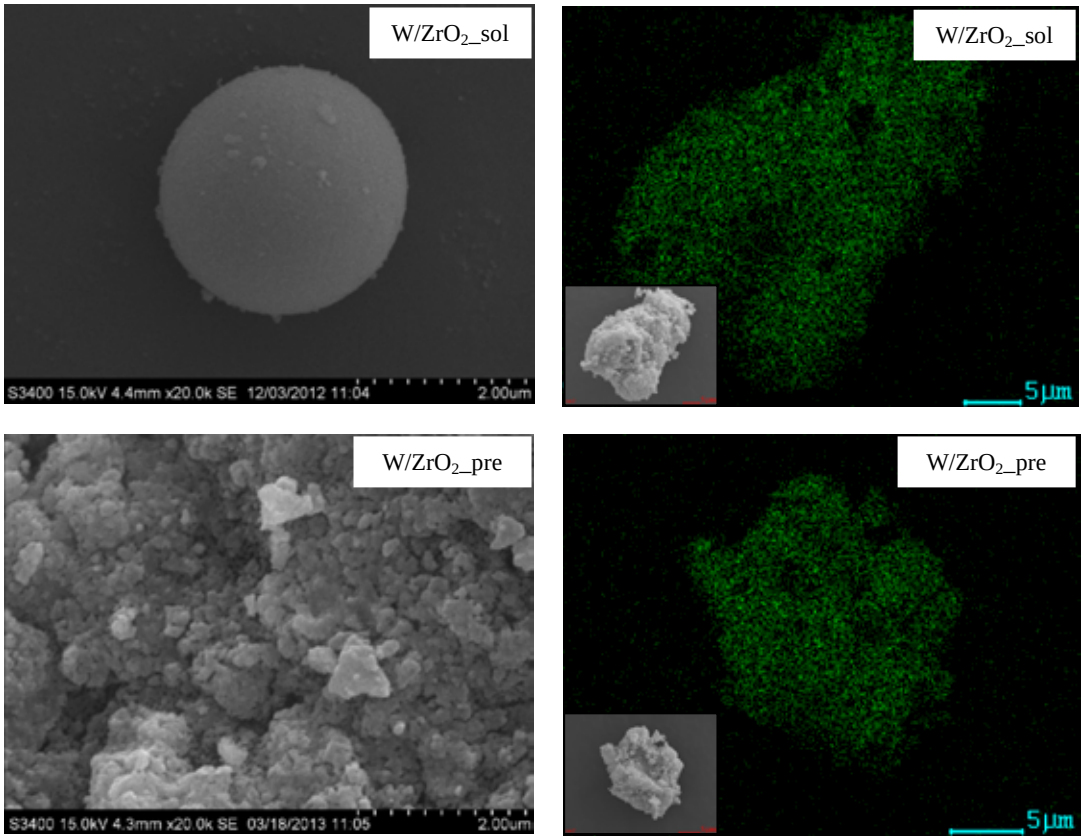

Figure 5.4 SEM micrograph for tungsten zirconia catalyst and EDX mapping for tungsten distributions.

The X-ray diffraction patteren of tungstated zirconia catalyst are shown in **Figure 5.4**. All tungstatated zirconia was prepared by impregnated with 15wt% of tungsten and calcined in air at 500^{o}C for 3 h. The XRD pattern shown the tetragonal phase at 30.4^{o}, 34.0^{o} and 50.3^{o} and monoclinic phase at 28.4^{o}, and 31.3^{o} Diffraction peaks of WO_3 crystallites were observed at 23.7 which conform with crystalline WO_3 by peak 2θ~23-25^{o} [43] illustrated that W/ZrO_2_sol and W/ZrO_2_pre are agglomerated of tungsten species on the surface of ZrO_2.

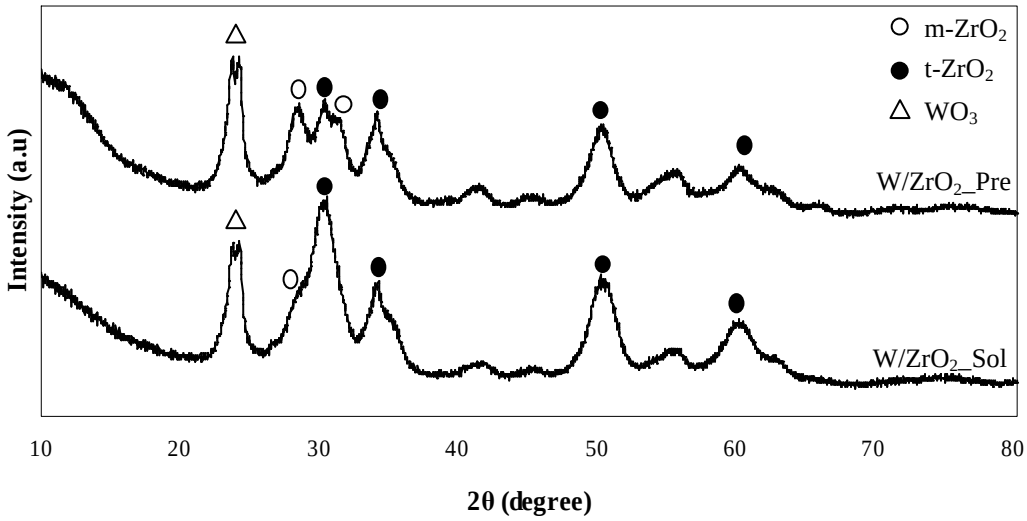

Figure 5.5 XRD patterns of the W/ZrO_2 prepared by the solvothermal and precipitation

The Raman spectra of W/ZrO_2 catalyst are shown in **Figure 5.6**. In addition, tungsten oxide are generally found at the 700-1400 cm^{-1} region. All the characteristic peak of tungsten species are shifted from 954.4 cm^{-1} (W/ZrO_2_sol) and 962.1 cm^{-1} (W/ZrO_2_pre) for W=O terminal in hydrated WO_x [17, 44]. Crystalline WO_3 shows characteristic Raman bands at 806.5 cm^{-1} (W/ZrO_2_sol) and 806.1 cm^{-1} (W/ZrO_2_pre) [43] which is conformed with the XRD result, where independent peaks due to crystalline WO_3 was observed.

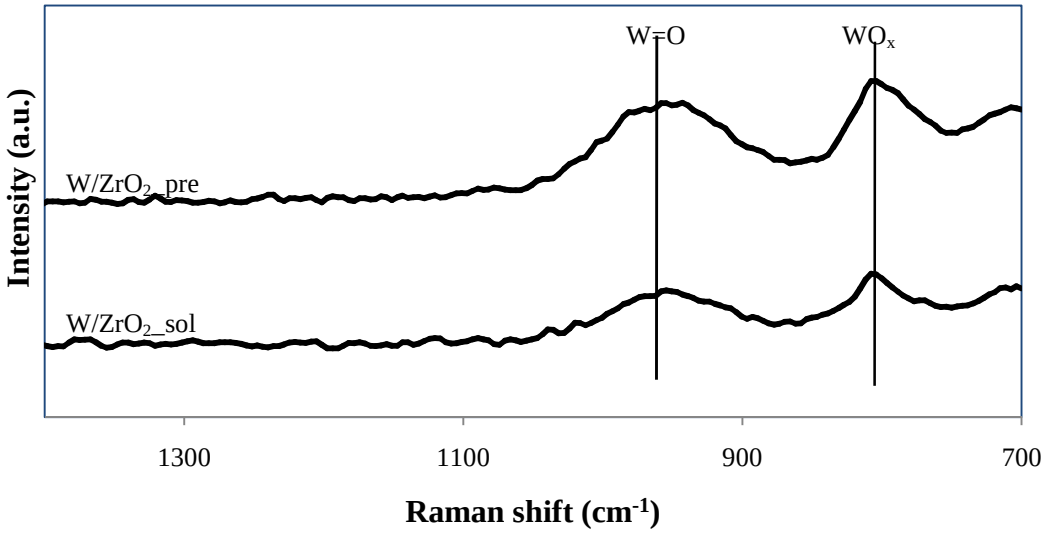

Figure 5.6 Raman spectra of various W/ZrO_2.

The characteristic of tungsted zirconia catalyst are shown in **Table 5.2**.The BET surface areas of the tungsteted zirconia catalyst were less than zirconia support. The result suggested that tungsten was deposited in some of pores of zirconia. This loss of surface area is significantly inhibited by the present of WO_x species or the emergence of monoclinic zirconia [8, 18]. The tungsten surface density of the catalyst was calculated from the WO_3 loading content. The W surface coverage of W/ZrO_2_pre sample can be achieved at the density of 3.06 W atom/nm^2, which less than that of W/ZrO_2_sol at 4.11 W atom/nm^2.

The acidity of tungstated zirconia catalyst samples were determined by using titration technique. The result revealed that W/ZrO_2_sol catalyst showed the highest surface acidity. This result conform with earlier work, which the generation of new acid sites increaseddue to interaction and dispersion of WO_x on the surface of the support [27].

Table 5.2 Physicochemical properties of W/ZrO_2 catalyst

Sample	BET surface area (cm^3/g)	Crystallite Size [a] (nm)	W surface density [b] (W atom/ nm^2)	Surface acidity (µmol/g)	XRD phase
W/ZrO_2_Sol	119.52	2.2	4.11	95	m-ZrO_2, t-ZrO_2, WO_3
W/ZrO_2_Pre	160.48	4.7	3.06	86	m-ZrO_2, t-ZrO_2, WO_3

[a] Calculation of crystallite size by Debye-Scherrer equation

[b] Measured by Ion-Exchange and titration with 0.05N NaOH

The esterification of acetic acid with methanol was carried out over the W/ZrO_2 catalysts with two preparation methods; solvothermal and precipitation at 60^oC The conversions of acetic acid are shown as a function of time in **Figure 5.7**. The result shows that the W/ZrO_2_pre catalyst are especially high activities than W/ZrO_2_sol. One of the possible reasons is that the higher BET surface area of W/ZrO_2_pre and W surface density content. It is well known that the W surface density content of catalysts and the formation of WO_x surface species is an essential factor for remaining the acidity of the catalyst, which may greatly influence the catalytic activity. Probably as a result of the generation of new acid sites due to interaction and dispersion of WOx on the surface of the support.

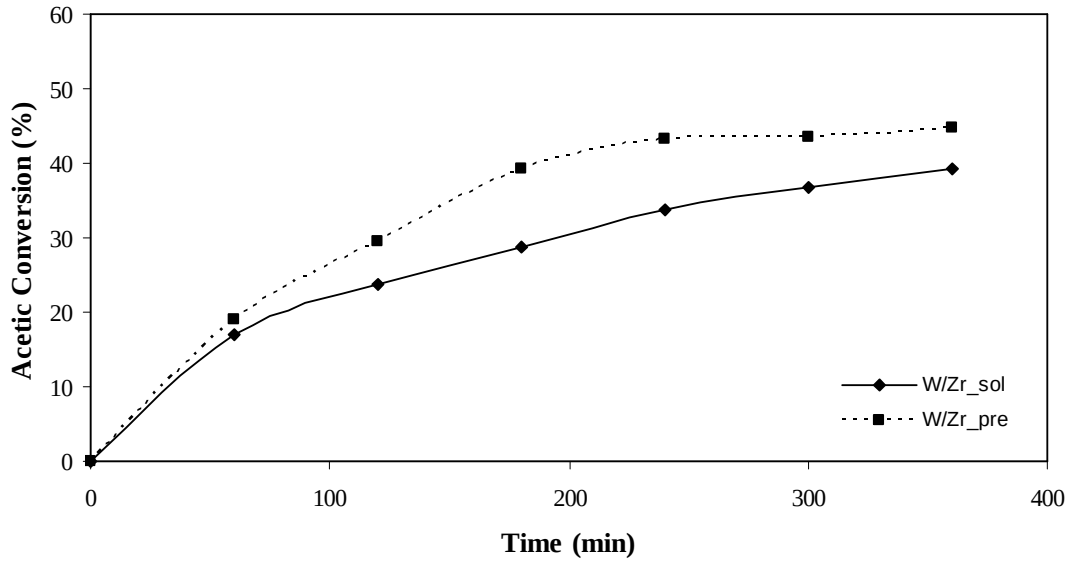

Figure 5.7 Catalytic activities on the different W/ZrO_2 catalyst.

5.2 Characteristics of Ga modified ZrO_2 support for W/ZrO_2 catalyst.

This work has been focued on the effect of gallium modified on ZrO_2 support and investigated the effect of the activity of W/ZrO_2 on the esterification.

The SEM image in Figure 5.6 shows that gallium distributed on the zirconia support. The morphology of the zirconia after impregnated with gallium was still spherical shape in solvothermal preparation and irregular shape particle in precipitation preparation. There was no significant different in the wt% of 1wt% and 0.5wt%.

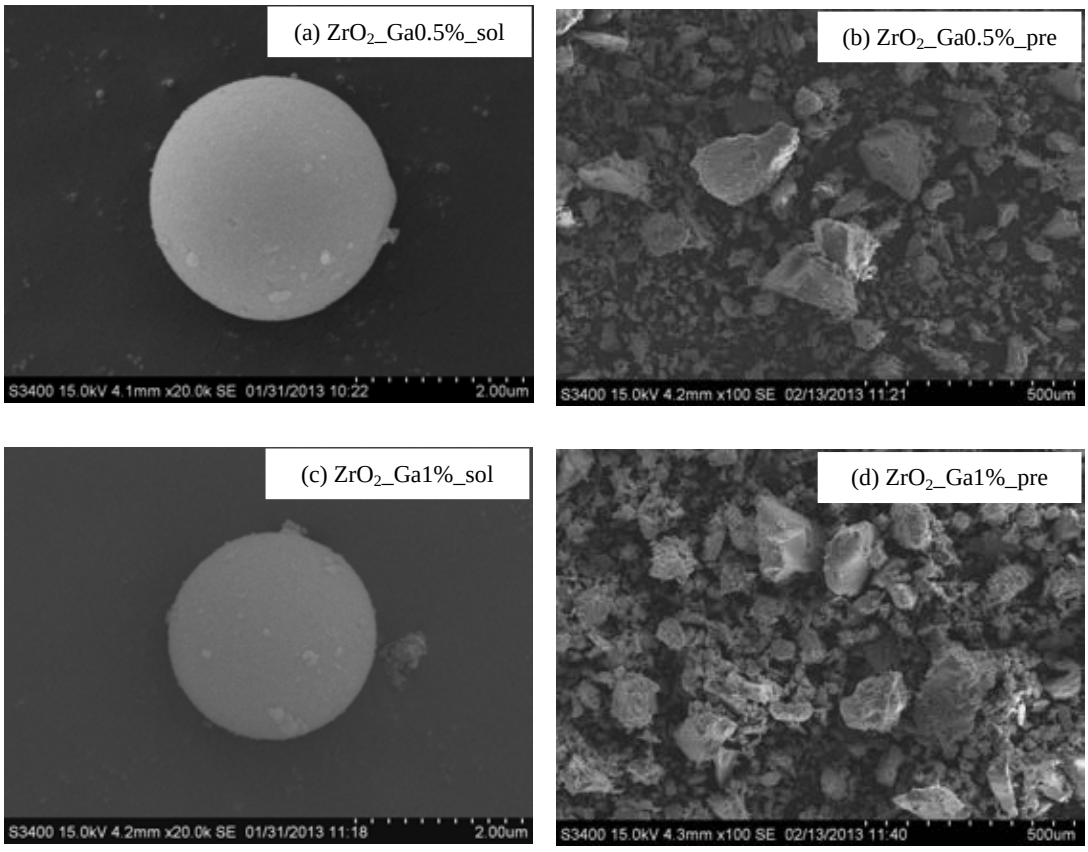

Figure 5.8 SEM micrographs of (a) ZrO_2_Ga0.5%_sol and (b) ZrO_2_Ga0.5%_pre (c) ZrO_2_Ga1%_sol and (d) ZrO_2_Ga1%_pre

The XRD patterns in **Figure 5.9** reveal two-phase formation of the crystalline zirconia phase as tetragonal crystalline zirconia phase (t-ZrO_2) and monoclinic zirconia phase (m-ZrO_2). There was no other crystalline phase. The average crystallite size calculated from the XRD line broadening using the Scherrer equation and the BET surface area of the zirconia are reported in the Table 5.3. The average crystallite size of zirconia were 2.5-2.8 nm for solvothermal and 1.2-1.5 nm for precipitation. The BET surface area increase in the order of ZrO_2_Ga1%_pre > ZrO_2_Ga0.5%_pre > ZrO_2_Ga1%_sol >ZrO_2_Ga0.5%_sol. It can be seen that the BET surface area and surface acidity show higher than the unmodified samples.

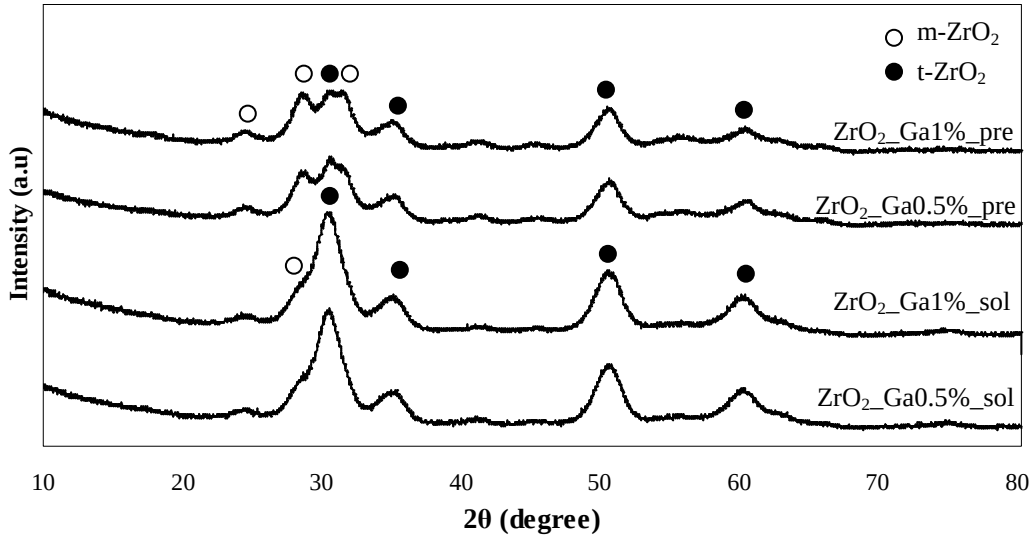

Figure 5.9 XRD patterns of ZrO_2 modified by Ga 0.5wt% and 1wt%

Table 5.3 Physicochemical properties of ZrO_2 modified with gallium.

Sample	**BET surface area (cm^3/g)**	**Crystallite Size [a] (nm)**	**Surface acidity (μmol/g)**	**[b]XRD Phase**
ZrO_2_ Ga0.5%_Sol	147.60	2.8	52	m-ZrO_2, t-ZrO_2
ZrO_2_ Ga1.0%_Sol	146.55	2.5	57	m-ZrO_2, t-ZrO_2
ZrO_2_ Ga0.5%_Pre	191.32	1.2	50	m-ZrO_2, t-ZrO_2
ZrO_2_ Ga1.0%_Pre	205.87	1.5	60	m-ZrO_2, t-ZrO_2

[a] Calculate of crystallite size by Debye-Scherrer equation

[b] Measured by Ion-Exchange and titration with 0.05N NaOH

After modified with Ga by impregnated 0.5wt% and 1wt%, the zirconia support was impregnated with 15wt% of tungsten and calcined in air at 500^{o}C for 3 h. The elemental distribution was also performed using SEM/EDX mapping on the external surface. **Figure 5.10** shows the Ga distribution in the support. All samples exhibited good distributions of Ga by without any change in the morphology. The W was also still good distributions on the zirconia.

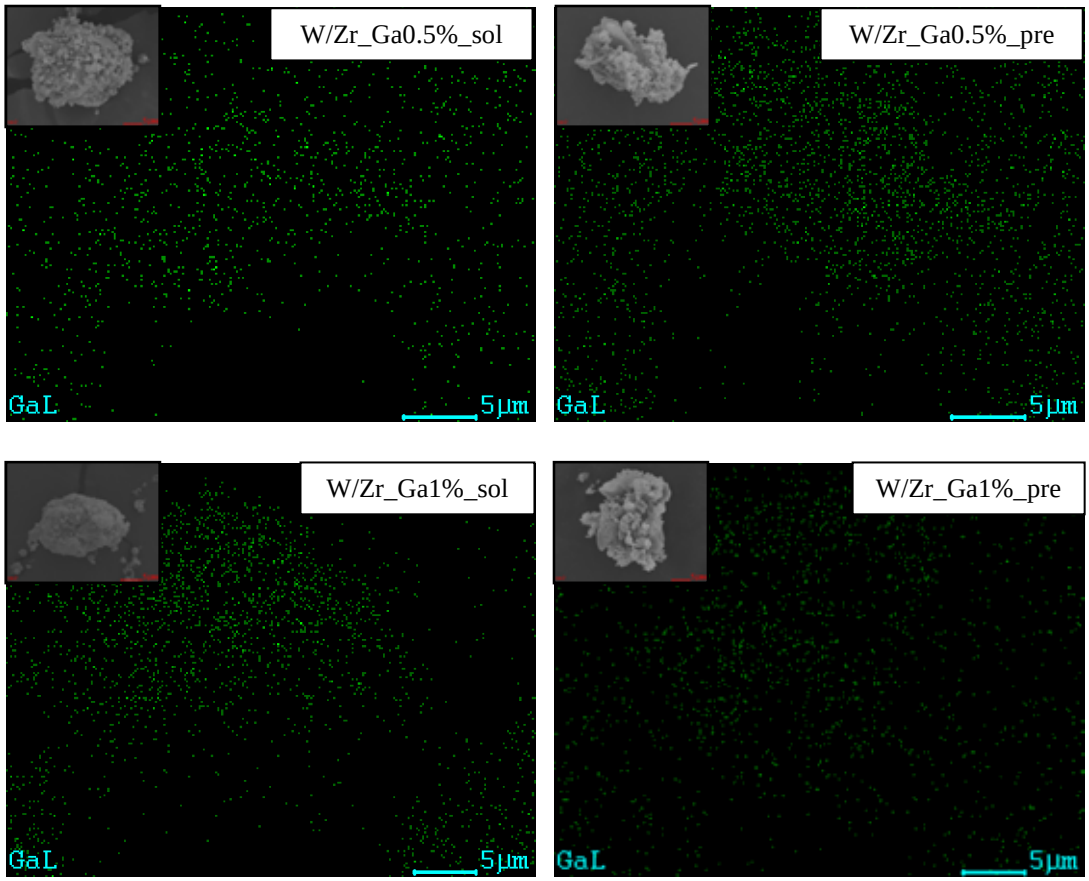

Figure 5.10 SEM micrograph for tungsten zirconia catalyst and EDX mapping for gallium distributions.

In **Figure 5.11**, the impregnated Ga on tungsten zirconia was also allowing to present a fraction of tetragonal crystalline zirconia phase (t-ZrO_2) and monoclinic zirconia phase (m-ZrO_2). The XRD patterns shows the tetragonal phase at 30.4^o, 34.0^o and 50.3^o and monoclinic phase at. 28.4^o, and 31.3^o The diffraction peaks of WO_3 crystallites were observed for all samples, indicating that tungsten oxide was agglomeration and low dispersion of tungsten species on zirconia.

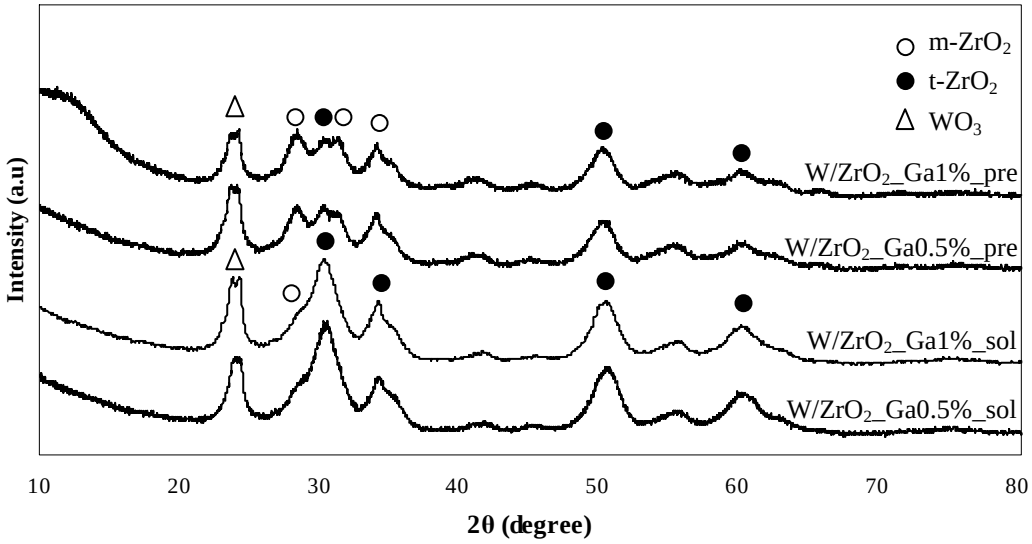

Figure 5.11 XRD patterns of W/ZrO_2 modified by Ga 0.5wt% and 1wt%

A more detail assessment of tungstate structure was identify by using Raman spectroscopy. **Figure 5.12** shows the Raman spectra for samples W/ZrO_2_ Ga0.5%_sol, W/ZrO_2_Ga1%_sol, W/ZrO_2_Ga0.5%_pre and W/ZrO_2_Ga1%_pre. The result reveal that smaller WO_3 crystallites are detectable by Raman which are good agreement with XRD result. The emergence of WO_3 evident by peaks at 802.5-806.8 cm^{-1} for all samples. Another broad band is W=O at 955.5-959.4 cm^{-1}.

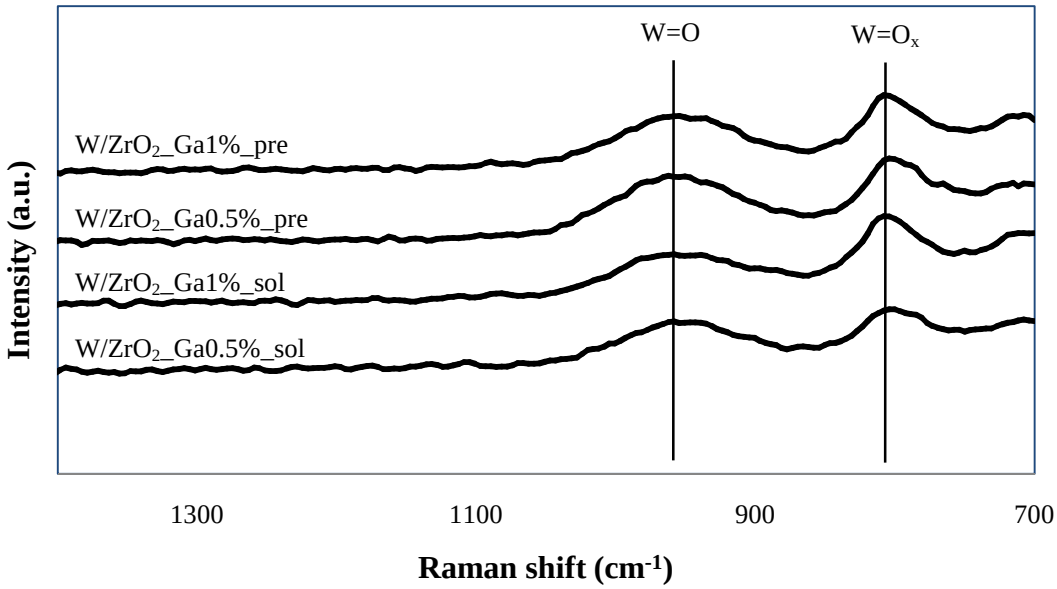

Figure 5.12 Raman spectra of various W/ZrO_2 catalyst.

Table 5.4 compares the catalytic properties of tungsten zirconia catalysts. The BET surface area was reduced from ZrO_2 support due to the penetration of tungsten species into the pore of ZrO_2 and probably that the tungsten oxide (WO_3) species blocked the pores of ZrO_2. The total acidities of W/ZrO_2_GaX catalysts at different wt% and preparation are summarized in **Table 5.4.** It can be seen that the total acidity of W/ZrO_2_Ga0.5%_sol, W/ZrO_2_Ga1%_sol, W/ZrO_2_Ga0.5%_pre and W/ZrO_2_Ga1%_pre are 110, 123, 103 and 115 μmol/g, respectively. Increasing the wt% results in the increased acidities. This suggests that the total acidity for the sample modified with Ga is much greater than the pure zirconia.

Table 5.4 Physicochemical properties of W/ZrO_2 modified with gallium.

Sample	BET surface area (cm^3/g)	Crystallite Size [a] (nm)	Surface acidity [b] (μmol/g)	XRD phase
W/ZrO_2_ Ga0.5%_Sol	-	2.3	110	m-ZrO_2, t-ZrO_2,WO_3
W/ZrO_2_ Ga1.0%_Sol	127.77	2.2	123	m-ZrO_2, t-ZrO_2,WO_3
W/ZrO_2_ Ga0.5%_Pre	148.87	0.9	103	m-ZrO_2, t-ZrO_2,WO_3
W/ZrO_2_ Ga1.0%_Pre	146.03	0.8	115	m-ZrO_2, t-ZrO_2,WO_3

[a] Calculate of crystallite size by Debye-Scherrer equation

[b] Measured by Ion-Exchange and titration with 0.05N NaOH

Figure 5.13 shows the catalytic activity. The esterification of acetic acid and methanol was carried out over the catalyst of W/ZrO2_Ga1%_pre, W/ZrO2_Ga0.5%_pre, W/ZrO2_Ga1%_sol and W/ZrO2_Ga0.5%_sol at 60oC. In the conversions of acetic acid after 6 h of time on stream as a function of time. The W/ZrO2_Ga1%_pre catalyst showed high activities for esterification of acetic acid. This is due to the higher acidity present as observed from acid base titration technique. The result shows that the ratio of gallium impregnated on the zirconia support synthesis influencing on catalytic activity.

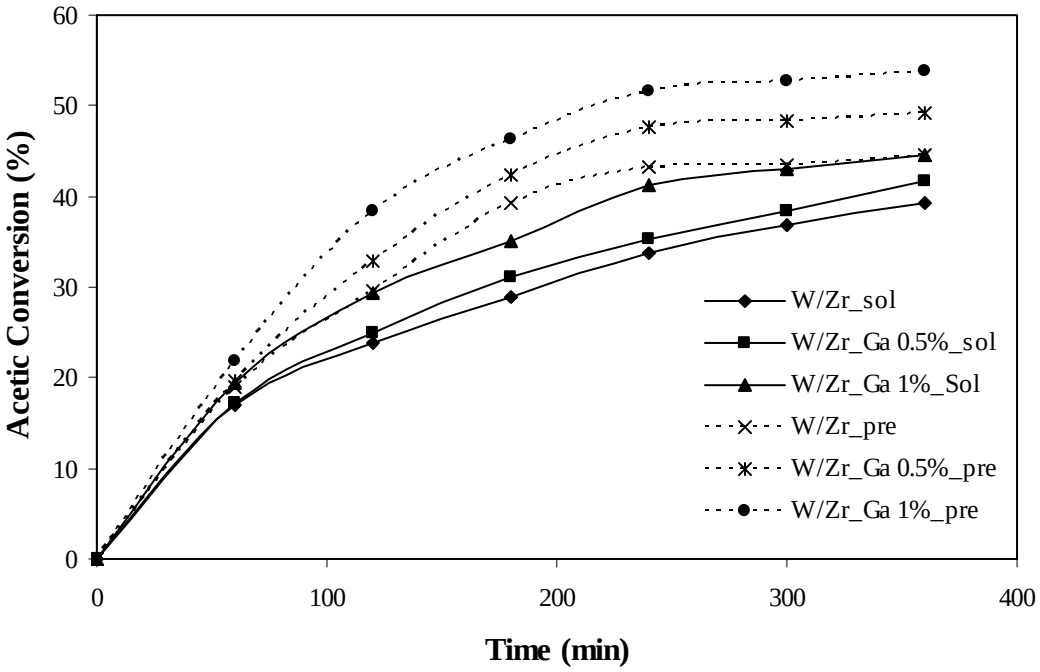

Figure 5.13 Catalytic activities on the different W/ZrO_2 catalyst.

5.3 Characteristics of B modified ZrO_2 support for W/ZrO_2 catalyst.

This work has been focused on the effect of boron modified on ZrO_2 support and investigated the effect of the activity of W/ZrO_2 on the esterification.

The effect B addition on the properties of zirconia in the ZrO_2_B1%_pre, ZrO_2_B0.5%_pre, ZrO_2_B1%_sol and ZrO_2_B0.5%_sol were further confirmed by SEM analysis. **Figure 5.14** shows the SEM images of all boron modified zirconia support. Based on SEM result, there was no change in the morphology of the zirconia after impregnated with B and no significant different in wt% of impregnated. Modified zirconia prepared by the solvothemal method still have a spherical shape and dence mass while in modified zirconia prepared by precipitation have irregularly shape particle.

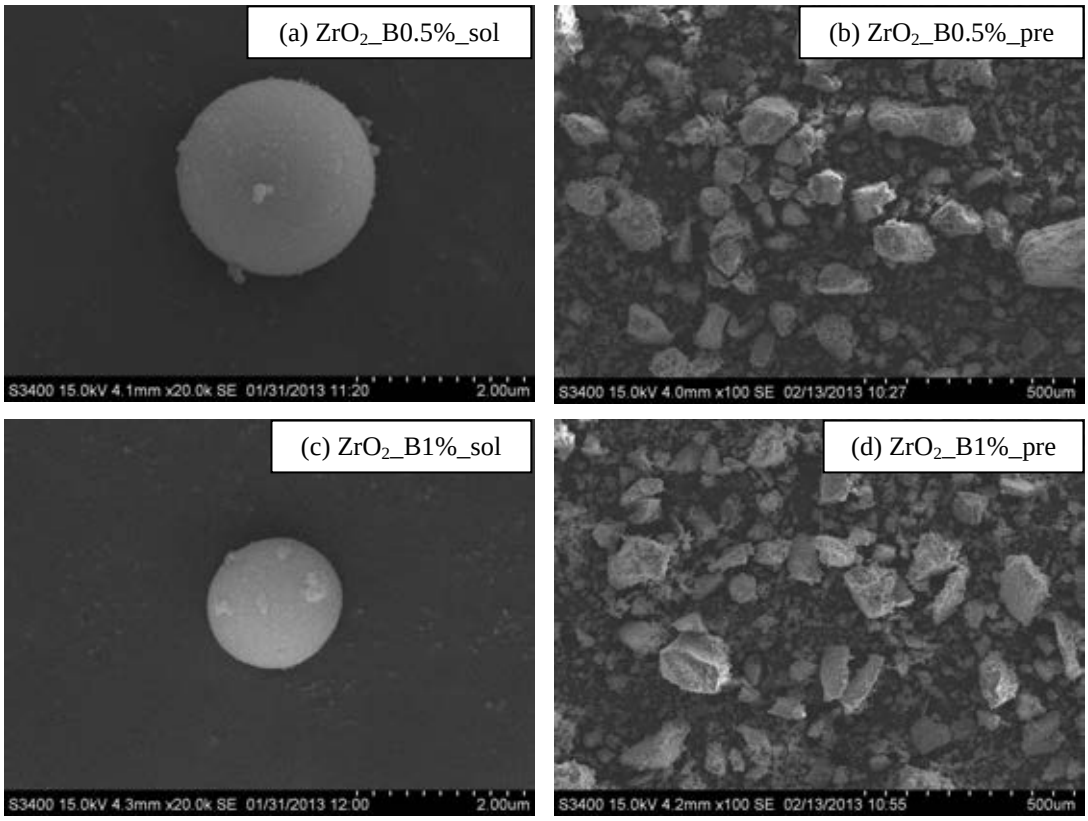

Figure 5.14 SEM micrographs of (a) ZrO_2_B0.5%_sol and (b) ZrO_2_B0.5%_pre (c) ZrO_2_B1%_sol and (d) ZrO_2_B1%_pre

The XRD patterns of ZrO_2_B1%_pre, ZrO_2_B0.5%_pre, ZrO_2_B1%_sol and ZrO_2_B0.5%_sol samples are shown in **Figure 5.15**. All the samples revealed similar XRD patterns indicating the primary tetragonal phase of zirconia (t-ZrO_2) at 2θ diffraction peaks at 30.2^o, 35.3^o and 50.6^o and monoclinic phase (m- ZrO_2) peaks at 24.3^o, 28.3^o and 31.4^o. The catalyst texural properties determined by the BET method and acid site concentrations as measured by ionexchange titration are listed in **Table 5.5.** It can be seen that the BET surface area and surface acidity of modified by boron show higher than the unmodified samples.

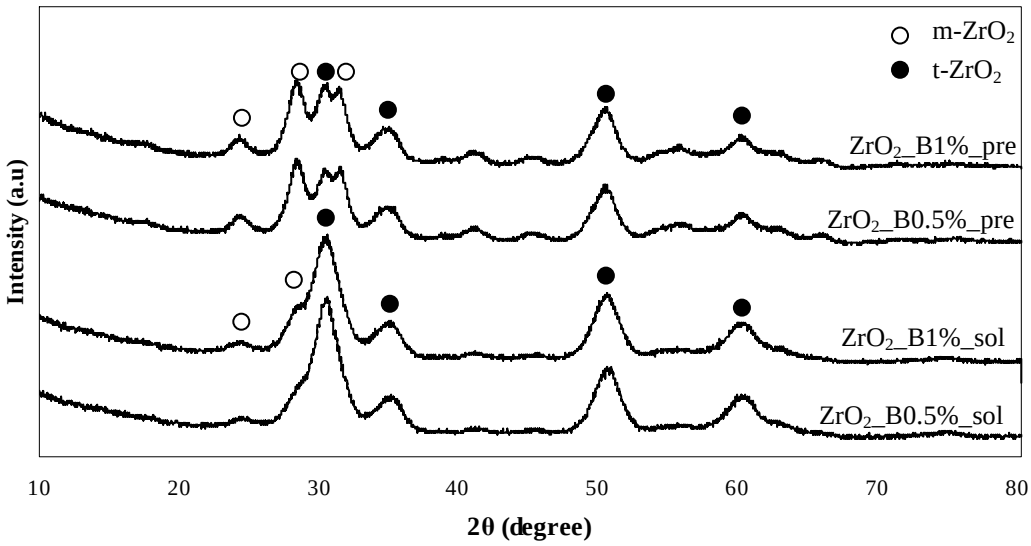

Figure 5.15 XRD patterns of ZrO_2 modified by B 0.5wt% and 1wt%

Table 5.5 Physicochemical properties of ZrO_2 modified with boron.

Sample	BET surface area (cm^3/g)	Crystallite Size [a] (nm)	Surface acidity [b] (µmol/g)	XRD Phase
ZrO_2_ B0.5%_Sol	130.89	3.0	50	m-ZrO_2, t-ZrO_2
ZrO_2_ B1.0%_Sol	153.83	2.4	57	m-ZrO_2, t-ZrO_2
ZrO_2_ B0.5%_Pre	159.67	1.7	54	m-ZrO_2, t-ZrO_2
ZrO_2_ B1.0%_Pre	157.35	1.7	58	m-ZrO_2, t-ZrO_2

[a] Calculate of crystallite size by Debye-Scherrer equation

[b] Measured by Ion-Exchange and titration with 0.05N NaOH

Figure 5.16 shows the XRD patterns of W/ZrO_2 which was impregnate by boron 1wt% and 0.5%wt on two preparation method. The characteristic diffractions of monoclinic zirconia (m-ZrO_2) are obvious, while the tetragonal phase is still dominant. These bands indicated that microcrystalline WO_3 is formed on the surface of W/ZrO_2 catalyst.

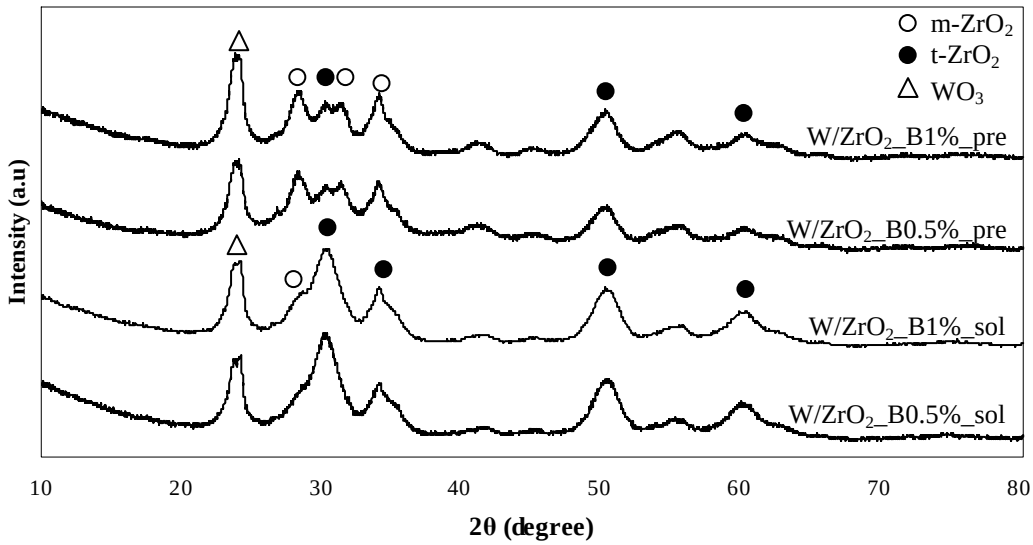

Figure 5.16 XRD patterns of W/ZrO_2 modified by B 0.5wt% and 1wt%

The Raman spectra of various W/ZrO_2 catalyst are shown in **Figure 5.17**. Raman spectroscopy was used to identify molecular level structural change in the tungsten oxide over layer under different preparation and %wt impregnated of boron. All the characteristic of tungsten species shifted for W=O terminal and hydrated WO_x at peak 953.9-966.1 cm^{-1} and 802.2-807.2 cm^{-1} respectively.

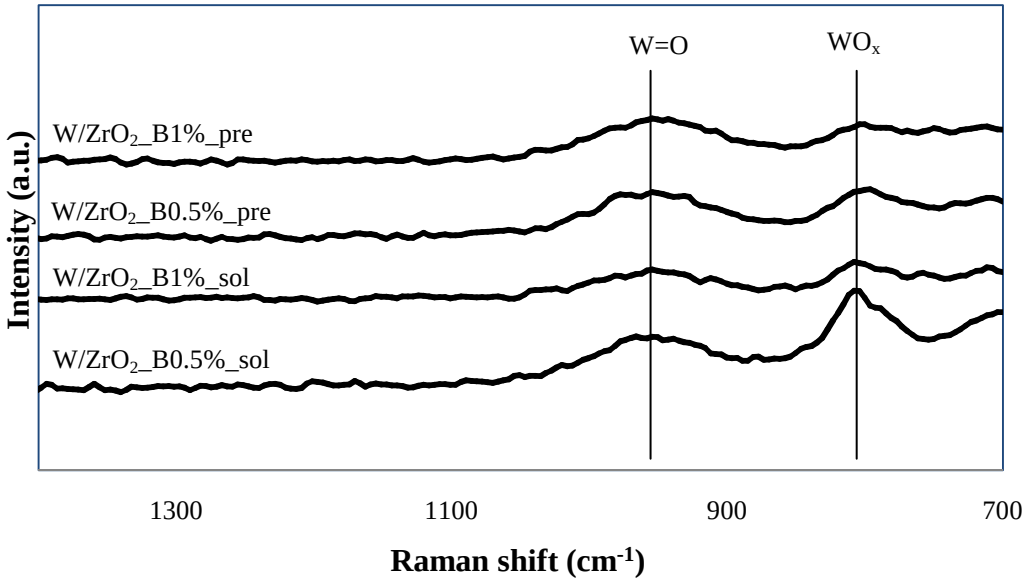

Figure 5.17 Raman spectra of various W/ZrO_2.

The SEM image in **Figure 5.18** revealed morphology of the zirconia after impregnated with boron. There were still spherical shape in solvothermal preparation and irregular shape particle in precipitation preparation. There was no significant different in the wt% of 1wt% and 0.5wt%. The tungsten was distribute on the surface of zirconia

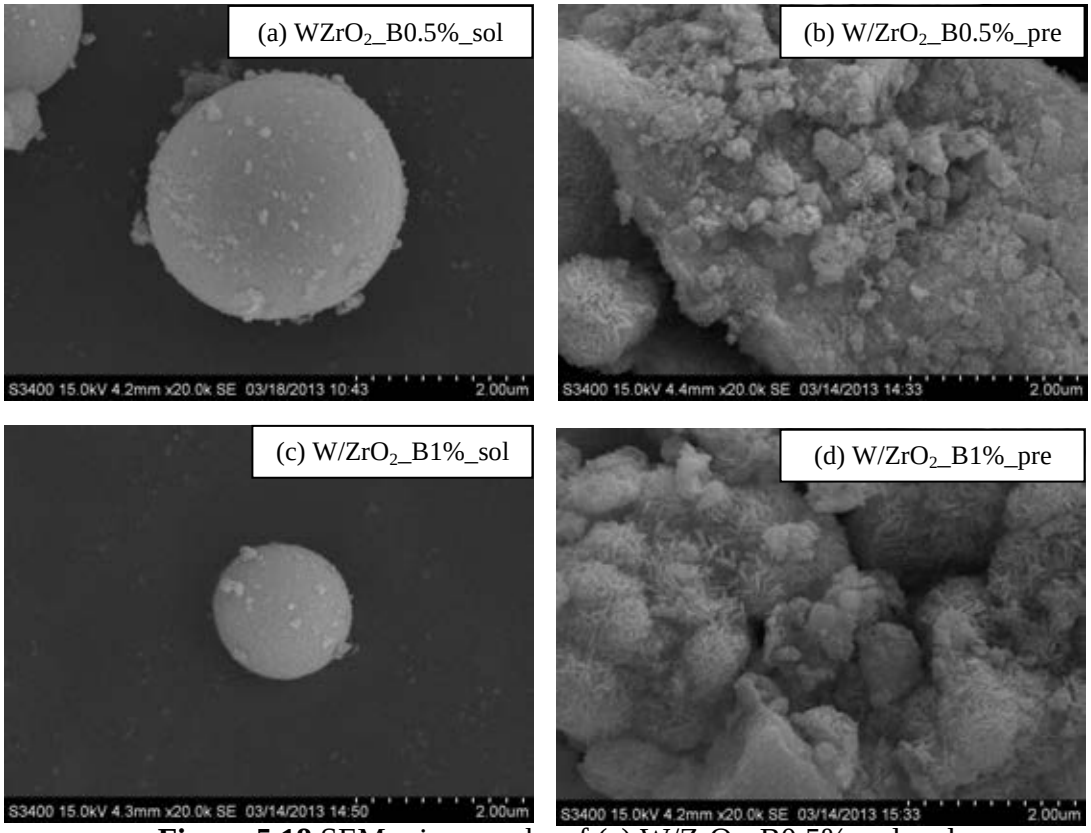

Figure 5.18 SEM micrographs of (a) W/ZrO_2_B0.5%_sol and (b) W/ZrO_2_B0.5%_pre (c) W/ZrO_2_B1%_sol and (d) W/ZrO_2_B1%_pre

The characteristics of various tungstated zirconia catalysts are shown in **Table 5.6,** In this study, the zirconia was impregnated with 0.5wt% and 1wt% of boron from HBO_3 acid and dried at 110^{o}C 24 h. After that, it was impregnated with 15wt% of tungsten and calcined in air at 500^{o}C for 3 h. The acidity of Tungsten zirconia catalyst samples were determined by using titration technique. The result revealed that W/ZrO_2_B0.5%_pre catalyst showed the highest surface acidity. By the way, the

Table 5.6 Physicochemical properties of W/ZrO_2 modified with boron.

Sample	Crystallite Size [a] (nm)	Surface acidity (µmol/g)	XRD phase
W/ZrO_2_ B0.5%_sol	2.4	72	m-ZrO_2, t-ZrO_2,WO_3
W/ZrO_2_ B1.0%_sol	2.0	57	m-ZrO_2, t-ZrO_2,WO_3
W/ZrO_2_ B0.5%_pre	0.8	74	m-ZrO_2, t-ZrO_2,WO_3
W/ZrO_2_ B1.0%_pre	0.8	62	m-ZrO_2, t-ZrO_2,WO_3

[a] Calculate of crystallite size by Debye-Scherrer equation

[b] Measured by Ion-Exchange and titration with 0.05N NaOH

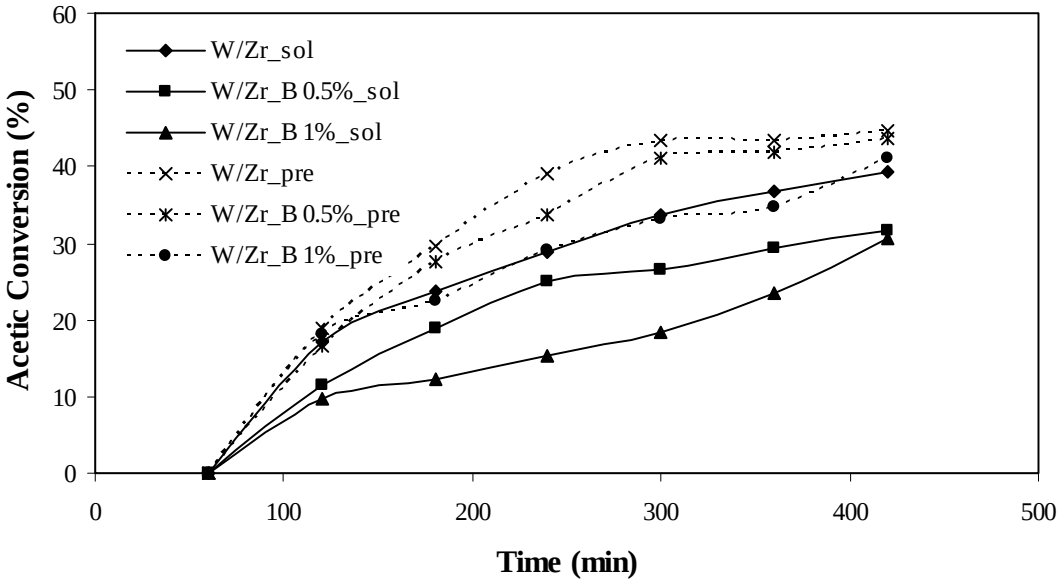

Figure 5.19 Catalytic activities on the different W/ZrO_2 catalyst.

Acetic acid conversions in the esterification reaction of acetic acis and methanol over four B modified tungstated zirconia catalysts and two regular tungstated zirconia catalyst as mentioned before are shown in **Figure 5.19** It indicated the increased conversion in the order of W/ZrO_2_pre >W/ZrO_2_ B0.5%_pre > W/ZrO_2_ B1%_pre > W/ZrO_2_sol >W/ZrO_2_ B0.5%_sol > W/ZrO_2_ B1%_sol.

It was observed that the conversion decreased in opposite trend with the increase of wt% boron. When the impregnated of boron is maximum for zirconia support, the

activity is decrease. It is conform with the number of surface acidity from acid-base titration techniques **(Table 5.6)** show decreased after impregnate with tungsten. One of the possible reasons is that the small atomic size of boron is able to interact with tungsten resulting in the decreased surface acidity.

CHAPTER VI

CONCLUSIONS AND RECOMMENDATIONS

6.1 Characteristics of zirconia support and W/ZrO_2 for preparation method of solvothermal and precipitation

This study compares characteristic of ZrO_2 and W/ZrO_2 catalyst of two preparation methods, such as the solvothermal and precipitation. The colour of zirconia are same white. The SEM image showed spherical and a dense mass of solvothermal while irregular and roughness shaped particles were observed in precipitation method. XRD and Raman spectroscopy result of W/ZrO_2 indicated that the W phase is present as a surface interaction species. Crystalline WO_3 was observed for both solvothermal and precipitation. The tungstated zirconia prepared by solvothermal as the support W/ZrO_2 result in the highest surface acidity. It revealed that the tungstated zirconia catalyst prepared by precipitation exhibited the highest activity due to high BET surface area and strength of acid site compare to that prepared by the solvothermal method.

6.2 Characteristics of Ga modified ZrO_2 support for W/ZrO_2 catalyst.

The gallium modified zirconia support with different at 0.5wt% and 1.0wt% of Ga from $GaNO_3$. The gallium shows good distributions on zirconia support by without any change in the morphology. The acidity measurement of zirconia support revealed that the activity of 1wt% of gallium increased acidities than others. The XRD of zirconia Ga modified support has no significant different from normal preparation. For the W/ZrO_2 catalyst, XRD and Raman spectroscopy result of all sample impregnated indicated that the W=O terminal and crystalline WO_3 are present as a surface interaction species for all samples. The catalytic activity obtained from W/ZrO_2_Ga1%_pre is the highest due to the BET surface area and increased of acidity add in from gallium modification.

6.3 Characteristics of B modified ZrO_2 support for W/ZrO_2 catalyst.

The effect B from HBO_3 with 1wt% and 0.5wt% addition on the properties of zirconia support. There are no significant difference in spherical shape after impregnated boron on the support. The shape was still spherical in solvothermal and irregular dense mass in precipitation. BET surface of the zirconia are higher after impregnation with boron. However, the results after impregnation with tungsten showed the opposite trend. With boron loading at 1 wt%, the activity and surface acidity decreased than the unmodified one, affecting by the two preparation methods. The possible reason may be the small atomic size of boron is able to interact with tungsten resulting in the decreased surface acidity.

6.4 Recommendation

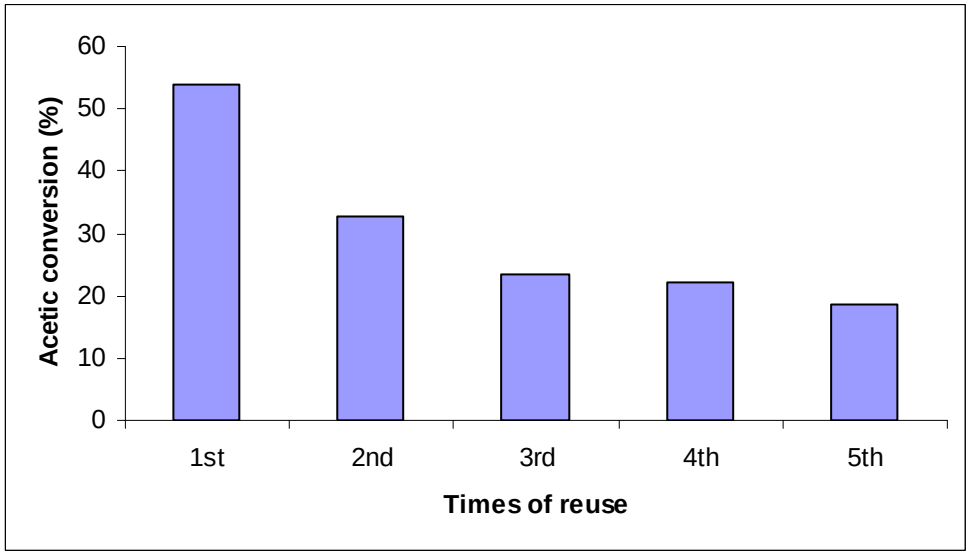

Figure 6.1 Acetic acid conversion of reusable catalyst (W/ZrO2_Ga1%_Pre)

The catalyst sample with the highest activities towards esterification (W/ZrO_2_Ga1%_pre) was selected to study the catalyst reusability. This study using esterification of acetic acid with methanol was carried out over the catalyst at 60^{o}C. After each 6 h cycle, the reaction mixture was cooled to room temperature and then

the solid catalyst was simply separated from the liquid mixture by centrifugation and a fresh reaction mixture was added. **Figure 5.20** shows the acetic acid conversion for five consecutive reaction cycles (without treatment) of W/ZrO_2_Ga1%_pre. The conversion of acetic acid decrease from 55% (first cycle) to 24%(fifth cycle). While forth cycle and fifth cycle are rarely stable. The decrease in the reaction rate may be attributed to W/ZrO_2_Ga1%_pre can be leached or deactivated mechanism.

Some ideas derived from this research are suggested here for the future research:

1. The effect of strong/weak acidity of Ga and B should be investigated
2. The effect of Bronsted and Lewis acidity of catalyst should be investigated.
3. The factor of deactivated/leaching of the reused catalyst including deactivation mechanism should be investigated.

REFERENCE

[1] Math, M.C., S.P. Kumar, and S.V. Chetty. Technologies for biodiesel production from used cooking oil. **Energy for Sustainable Development** 14 (2010) : 339-345.

[2] Raita, M., Laothanachareon, T., Champreda, V and Laosiripojana, N Biocatalytic. Biocatalytic esterification of palm oil fatty acids for biodiesel production using glycine-based cross-linked protein coated microcrystalline lipase. **Journal of Molecular Catalysis B: Enzymatic** 73 (2011) : 74-79.

[3] Shi W.and others, Continuous esterification to produce biodiesel by SPES/PES/ NWF composite catalytic membrane in flow-through membrane reactor. **Experimental and kinetic studies. Bioresource Technology** 129 (2013) : 100-107.

[4] Eterigho, E.J., J.G.M. Lee, and A.P. Harvey. Triglyceride cracking for biofuel production using a directly synthesised sulphated zirconia catalyst. **Bioresource Technology** 102 (2011) : 6313-6316.

[5] Sun, Y., Walspurger, S., Louis, B and Sommer, J. Investigation of factors influencing catalytic activity for n-butane isomerization in the presence of hydrogen on Al-promoted sulfated zirconia. **Applied Catalysis A: General** 292 (2005) : 200-207.

[6] Ni, J. and F.C. Meunier. Esterification of free fatty acids in sunflower oil over solid acid catalysts using batch and fixed bed-reactors. **Applied Catalysis A: General** 333 (2007) : 122-130.

[7] Brei V.V.and others, Superacid WOx/ZrO2 catalysts for isomerization of n-hexane and for nitration of benzene. **Studies in Surface Science and Catalysis** 2000 : 387-395.

[8] López D.E.and others, Esterification and transesterification using modified-zirconia catalysts. **Applied Catalysis A: General** 339 (2008) : 76-83.

[9] Zhang, S, Xian, John, W. Tierney, W and Irving, W. Tungstatae-modified zirconia as a hydroisomerization catalyst for high moleular weight linear parafins. **Applied Catalysis A: General** 377 (2006) : 69-73.

[10] Hwang, C.-C and Mou, Chung-Yuan. Enhanced catalytic activity for butane isomerization with alumina-promoted tungstated mesoporous zirconia. **Applied Catalysis A: General** 323 (2007) : 9-17.

[11] Zheng J.and others, Promoting effect of boron with high loading on Ni-based catalyst for hydrogenation of thiophene-containing ethylbenzene. **Catalysis Communications** 21 (2012) : 18-21.

[12] Usman, U., Takaki, M., Kubota, T., Okamoto, Y. Effect of boron addition on a MoO3/Al2O3 catalyst: Physicochemical characterization. Applied Catalysis A: General 286 (2005) : 148-154.

[13] Kwak B.S.and others, Hydrogen-rich gas production from ethanol steam reforming over Ni/Ga/Mg/Zeolite Y catalysts at mild temperature. **Applied Energy** 88 (2011) : 4366-4375.

[14] Kumar, N. and L.E. Lindfors. Synthesis, characterization and application of H-MCM-22, Ga-MCM-22 and Zn-MCM-22 zeolite catalysts in the aromatization of n-butane. **Applied Catalysis A: General** 147 (1996) : 175-187.

[15] Song Y.and others, Effect of crystallization mode of hydrous zirconia support on the isomerization activity of Pt/WO3–ZrO2. **Catalysis Today** 166 (2011) : 79-83.

[16] Zhang, J., Zhang, Y., Tierney, J. and Wender, I. Effect of Crystallization of Hydrous Zirconia on the Isomerization Activity of Pt/WO3-ZrO2. **Chinese Journal of Catalysis** 31 (2010) : 374-376.

[17] Kuba S.and others, Structure and properties of tungstated zirconia catalysts for alkane conversion. **Journal of Catalysis** 216 (2003) : 353-361.

[18] López D.E.and others, Esterification and transesterification on tungstated zirconia: Effect of calcination temperature. **Journal of Catalysis** 247 (2007) : 43-50.

[19] Rabindran Jermy B.and otheers, Optimizing preparative conditions for tungstated zirconia modified with platinum as catalyst for heptane isomerization. **Catalysis Today** 164 (2011) : 148-153.

[20] Kaucký D.and others, Effect of the particle size and surface area of tungstated zirconia on the WOx nuclearity and n-heptane isomerization over Pt/WO3–ZrO2. **Applied Catalysis A: General** 397 (2011). : 82-93.

[21] Parida, K.M., P.K. Pattnayak, and P. Mohapatra. Liquid phase mononitration of chlorobenzene over WOx/ZrO2: A study of catalyst and reaction parameters. **Journal of Molecular Catalysis A: Chemical** 206 (2006) : 35-42.

[22] Sakthivel, R., H. Prescott, and E. Kemnitz. WO3/ZrO2: a potential catalyst for the acetylation of anisole. **Journal of Molecular Catalysis A: Chemical** 223 (2004) : 137-142.

[23] Ramu S.and others, Esterification of palmitic acid with methanol over tungsten oxide supported on zirconia solid acid catalysts: effect of method of preparation of the catalyst on its structural stability and reactivity. A**pplied Catalysis A: General** 276 (2004) : 163-168.

[24] Karim, A.H., Triwahyono, S., Jalil, A.A. and Hattori, H. WO3 monolayer loaded on ZrO2: Property–activity relationship in n-butane isomerization evidenced by hydrogen adsorption and IR studies. **Applied Catalysis A: General** 433-434 (2012) : 49-57.

[25] Chen S.and others, Thiolation of dimethyl sulfide to methanethiol over WO3/ZrO2 catalysts. **Journal of Molecular Catalysis A: Chemical** 365 (2012) : 60-65.

[26] Kourieh, R., Rakic, V., Bennici, S. and Auroux, A. Relation between surface acidity and reactivity in fructose conversion into 5-HMF using tungstated zirconia catalysts. **Catalysis Communications** 30 (2013) : 5-13.

[27] Wongmaneenil, P., B. Jongsomjit, and P. Praserthdam. Influence of calcination treatment on the activity of tungstated zirconia catalysts towards esterification. **Catalysis Communications** 10 (2009) : 1079-1084.

[28] Osiglio, L. and M. Blanco. Effect of the Addition of Boric Acid to Zirconia Synthesized Employing Pore-forming **Agents. Procedia Materials Science** 1 (2012) : 491-498.

[29] Xu J.and others, Effect of boron on the stability of Ni catalysts during steam methane reforming. **Journal of Catalysis** 261 (2009) : 158-165.

[30] Tu X.and others, The Promoting Effect of Ga2O3 on a Pt/WO3/ZrO2 Catalyst for n-Heptane Isomerization. **Chinese Journal of Catalysis** 30 (2009) : p. 378-380.

[31] Hwang, C.-C. and C.-Y. Mou. Comparison of the promotion effects on sulfated mesoporous zirconia catalysts achieved by alumina and gallium. **Applied Catalysis A: General** 365 (2009) : 173-179.

[32] Kaivalchatchawal P.and others, Effect of Ga- and BCl3-modified silica-supported [t-BuNSiMe2(2,7-t-Bu2Flu)]TiMe2/MAO catalyst on ethylene/1-hexene copolymerization. **European Polymer Journal** 48(2012) : 1304-1312.

[33] Ávila, D.M. and E.N.S. Muccillo. Influence of some variables of the precipitation process on the structural characteristics of fine zirconia powders. **Thermochimica Acta** 256 (1995) : 391-398.

[34] Wang J.A.and others, Comparative study of nanocrystalline zirconia prepared by precipitation and sol–gel methods. **Catalysis Today** 68 (2001) : 21-30.

[35] Feng, S. and L. Guanghua. **Chapter 4 - Hydrothermal and Solvothermal Syntheses, Modern Inorganic Synthetic Chemistry.** X. Ruren. and others. Amsterdam: Elsevier, 2011

[36] Markus Niederberger, N.P. **Solvothrmal Synthesis London**: Springer, 1998.

[37] Li, G., Hong, Z., Yang, H and Li, D. Phase composition controllable preparation of zirconia nanocrystals via solvothermal method. **Journal of Alloys and Compounds** 532 (2012) : 98-101.

[38] Uchiyama, H., K. Takagi, and H. Kozuka. Solvothermal synthesis of size-controlled ZrO2 microspheres via hydrolysis of alkoxides modified with acetylacetone. **Colloids and Surfaces A: Physicochemical and Engineering Aspects** 403 (2012) : 121-128.

[39]“Esterification”. [Online]. Available: http://www.chemguide.co.uk/organicprops/alcohols/esterification.html

[40] Wilson K.and others. **Novel supported solid acid catalysts for environmentally friendly organic synthesis, in Studies in Surface Science and Catalysis, F.V.M.S.M. Avelino Corma and G.F.** José Luis. Elsevie, 2011

[41] “Bronsted and Lewis". [Online]. Available http://www.scribd.com/doc/119496782/71113470-Organic-Chemistry-Kimberly-Carter.

[42] Kongwudthiti, S., Praserthdam, P., Silveston, P and Inoue, M. Influence of synthesis conditions on the preparation of zirconia powder by the glycothermal method. **Ceramics International** 29 (2003) : 807-814.

[43] Boyse, R.A. and E.I. Ko. Commercially available zirconia–tungstate as a benchmark catalytic material. **Applied Catalysis A: General** 177 (1999) : L131-L137.

[44] Hui, S.W. and J.A. Rayne. Doppler-shifted acoustic cyclotron resonance in tungsten. **Journal of Physics and Chemistry of Solids** 33 (1972) : 611-621.

APPENDICES

APPENDIX A

PREPARATION ZIRCONIA BY SOLVOTHERMAL

Preparation of ZrO_2 nanocrystal with solvothermal method are shown as below.

Reagent - Zirconium n-butoxide (MW = 327.56) 30 g
- 1,4-butanediol (MW = 90) 100g for mixed + 30 g for add in the tube.

The equipment for the synthesis of zirconia consists of an autoclave reactor as shown in Figure A.1. A temperature program controller was connected to a thermocouple attached to the autoclave.

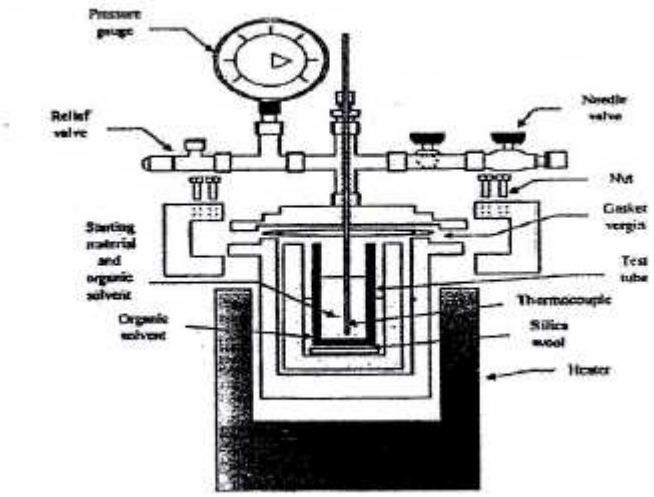

Figure A.1 Auto clave

APPENDIX B

PREPARATION ZIRCONIA BY PRECIPITATION

Preparation of ZrO_2 nanocrystal with precipitation method are shown as below.

Reagent - Zirconyl nitrate (MW = 231.23)
prepare (0.15M) = 34.68 g/1000 ml of DI
- Ammonia hydroxide (MW = 35.14) prepare (2.5wt%) = 2.5g/97.5g of DI

Zirconyl nitrate [$ZrO(NO_3)_2$] (0.15M) was carried out by slowly adding a solution into a well-stirred precipitation solution of ammonia hydroxide (NH_4OH) (2.5wt%) at room temperature. The pH of the solution was carefully controlled at 10.

APPENDIX C

CALCULATION FOR GA AND B MODIFTED ZIRCONIA

Calculation for the Ga modified on zirconia support.

Reagent

- Gallium (III) nitrate hydrate ($Ga(NO_3)$) (MW = 131.72)
- Gallium (Ga) (MW=69.72)

- Boric acid ($H_3BO_{3)}$ (MW = 61.83)
- Boron (B) (MW=10.82)

Example : prepare 1wt% of Ga by use zirconia support 5 g

For 5 g of zirconia support,

$$\text{Galium(III) nitraye required} = 5 \text{ x } \frac{1}{(100-1)}$$

$$= 0.05 \text{ g}$$

Tungsten 0.05 g prepare from $GaNO_3$

$$GaNO_3 = \frac{\text{MW of GaNO3 xGa required}}{\text{MW of Ga}}$$

$$= (131.72\text{x}0.05)/(69.72)$$

$$= 0.0935 \text{ g}$$

APPENDIX D

CALCULATION FOR CATALYST PREPARATION

Calculation for the precipitation of Tungsten(VI) Chloride loading catalyst (15%W/ZrO_2)

Reagent

- Tungsten hexachloride (WCl_6) MW = 396.56
- Tungsten (W) MW = 183.56
- Zirconia (ZrO2) MW = 85

Calculation:

For 2 g of zirconia support,

$$\text{Tunsten required} = 2 \text{ x } \frac{15}{(100-15)}$$

$$= 0.353 \text{ g}$$

Tungsten 0.353 g prepare from WCl_6

$$WCl_6 = \frac{\text{MW of } WCl_6 \text{ x W required}}{\text{MW of W}}$$

$$= (396\text{-}0.353)/(183.56)$$

$$= 0.763 \text{ g}$$

APPENDIX E

CALCULATION FOR CRYSTALLITE SIZE

The calculation crystallite size by Dedye-Scherrer equation

The crystallite size was calculated from the half-height width of the diffraction peak of XRD pattern using the Debye-Scherrer equation.

From Scherrer equation: $D = \frac{K\lambda}{\beta \cos\theta}$

Where D = Crystallite size, Å

K = Crystallite-shape factor (=0.9)

λ = X-ray wavelength (1.5418 Å for CuK_{α})

θ = Observed peak angle, degree

β = X-ray diffraction broadening, radian

The X-ray diffraction broadening (β) is the pure width of power diffraction free from all broadening due to the experimental equipment. α-Alumina is used as a standard sample to observe the instrumental broadening since its crystallite size is larger than 2000 Å. The X-ray diffraction broadening (β) can be obtained by using Warren's formula. B^2_M

Warren's formula $\beta = \sqrt{B_M^2 - B_s^2}$

Where B_M = the measure peak width in radians at half peak height.

B_S = the corresponding width of the standard material.

APPENDIX F

CONDITION OF GAS CHROMOTROGRAPHY

The condition of Gas Chromatography (GC) analysis for this study

The concentration of reacted samples was determined using a SHIMADZU gas chromatography (GC-14B) equipped with Chrompack SE52 column and flame ionization. UHP N_2 was used as the carrier gas as presented in Table F.1

Table F.1 analysis condition of esterification of acetic acid and methanol

Gas Chromatography	**Shimadzu GC-14B**
Detector	FID
Column	Chrompack SE52
Carrier gas	N_2 (UHP grade)
Carrier gas flow rate (ml/min)	30
Injector temperature (^oC)	200
Detector temperature (^oC)	260
Column temperature	
Initial temperature (^oC)	60
Holding time (min)	2
Ramp rate (^oC/min)	10
Final temperature (^oC)	120
Holding time (min)	9

APPENDIX G

CALCULATION OF CATALYTIC PERFORMANCE

The catalytic performance for esterification of acetic acid and methanol was evaluated in term of percent acetic conversion.

$$\% \text{ Acetic acid conversion} = \frac{\text{initial acetic acid conc.} - \text{acetic acid conc at time}}{\text{initial actic acid conc}} \text{x}100$$

APPENDIX G

LIST OF PUBLICATION

Proceeding:

Chanidapa Padoongpitukchon and Bunjerd Jongsomjit, “Characteristic of Ga modified ZrO2 on W/ZrO2Catalysts for Esterification”, Proceeding of the RSU Research Conference 2013, Bankkok Thailand, April., 2013.

BIOGRAPHY

Miss Chanidapa Padoongpitukchon was born on March 28th, 1986 in Thailand. She graduated bachelor's degree from Srinakarinwirot University in the faculty of Chemical Engineering in 2008. After that, she studied master's degree at Chulalongkorn University, faculty of Chemical Engineering in 2010.

Turnitin

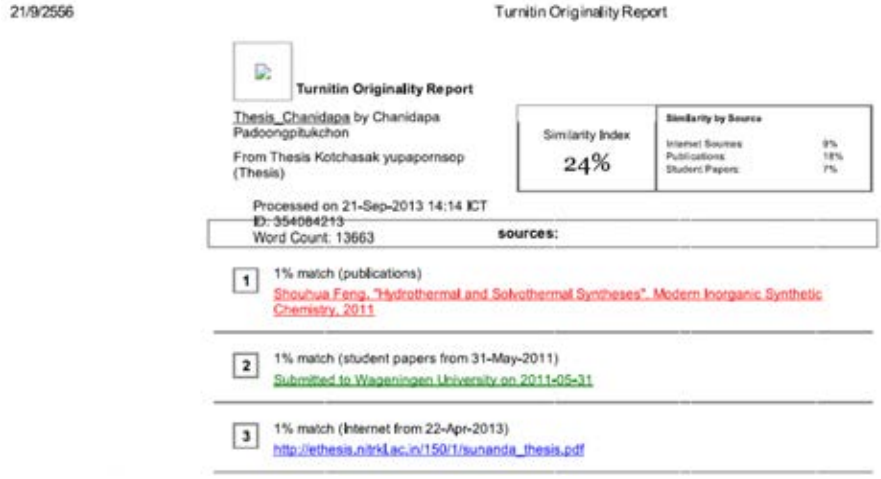

21/9/2556 Turnitin Originality Report

Turnitin Originality Report

Thesis_Chanidapa by Chanidapa Padoongpitukchon

From Thesis Kotchasak yupapornsop (Thesis)

Processed on 21-Sep-2013 14:14 ICT
ID: 354084213
Word Count: 13663

Similarity Index
24%

Similarity by Source
Internet Sources: 9%
Publications: 18%
Student Papers: 7%

sources:

1 1% match (publications)
Shouhua Feng, "Hydrothermal and Solvothermal Syntheses", Modern Inorganic Synthetic Chemistry, 2011

2 1% match (student papers from 31-May-2011)
Submitted to Wageningen University on 2011-05-31

3 1% match (Internet from 22-Apr-2013)
http://ethesis.nitrkl.ac.in/150/1/sunanda_thesis.pdf